PINSA, 64, A, No 3, May 1998, pp. 315-340.

EQUATORIAL AND LOW LATITUDE THERMOSPHERE-IONOSPHERE INTERACTION

R SRIDHARAN

Physical Research Laboratory, Ahmedabad 380 009, India
(E-mail : sridhar@prl.ernet.in)

(Received 04 December 1997 ; Accepted 22 January 1998)

Over the recent years the equational and low latitude phenomena in the upper atmosphere have been drawing the attention of Aeronomers and space scientists world-wide. The equatorial region reveals a variety of geophysical phenomena which are perfect examples for the neutral atmosphere and the F-region of the ionosphere to behave as a closely coupled system. The present paper is an overview of these interactive processes and our current understanding and it also touches upon the grey areas which call for a concerted investigation.

Key Words : Thermosphere-Ionosphere Interaction; Equatorial Aeronomy; Thermal Structure of the Upper Atmosphere; Equatorial Electrodynamics; Plasma Instability

Introduction

The thermosphere, which refers to that part of the upper atmosphere spanning from ~85km and extending to atleast 350-400km is unique in many ways. This is the region which extends from the coldest part around 85km (the mesopause) to the hottest part of the upper atmosphere (>350km - the exosphere) and this is where significant interaction of the solar EUV radiation results in the formation of the well-known ionosphere. The thermosphere thus encompasses the region of maximum production of ionisation within it. This is the region where the differential heating of the upper atmosphere results in neutral winds which in turn provides the mechanical energy for global scale dynamo action generating electric fields. These electric fields in turn are responsible for a variety of electrodynamical processes including several plasma instabilities peculiar to the specific geographical location. In addition to the above, the turbulent mixing of the atmospheric constituents in the lower atmosphere ceases in the lower thermosphere giving way to molecular diffusion higher above, which ensures diffusive equilibrium of the different atmospheric constituents depending upon their mass. Though the ionospheric densities are several orders of magnitude less than the neutral densities, the response of the ionosphere to the probing radio waves and the selective restraint imposed on them by the geomagnetic field, the ionized part of the upper atmosphere retains its own identity.

In general, irrespective of the geographical location, the neutral thermosphere and the F-region of the ionosphere are known to exist as a closely coupled system, to that effect, any change in the structural and dynamical parameters in one promptly gets reflected in the other. As a system, the TIS (Thermosphere-Ionosphere System) is coupled to other regions of the atmosphere in a variety of ways. For example, the magnetosphere is coupled electrically to the high latitude TIS along the highly conducting magnetic field lines, while the high and low latitudes are coupled by neutral dynamical and electrodynamical means. The former is through winds and waves while the latter is through the conducting ionosphere. The high-low latitude coupling is known to be extremely important during geomagnetically disturbed periods. This aspect will be dealt with in some detail later.

The lower and middle atmosphere extending upto 100km is also coupled to the upper regions viz., the thermosphere and the F-region of the ionosphere by neutral and electrodynamical forcings. Apart from this, the lower region acts as a source of waves that vertically propagate upwards altering the structure and energetics higher above, while it continuous to be the seat of dynamo action resulting in the generation of electric fields and the associated processes.

As a system, the TIS shows a large variability such as with altitude, latitude, longitude, local time, season, solar activity and also geomagnetic activity. These variations are an outcome of the couplings, time delays and feed back mechanisms that are inherent in the system, as well as from the effects of solar, interplanetary, magnetospheric as well as mesospheric processes.

The various driving processes mentioned above are known to act in concert to determine the density and temperature morphologies of the ionized and neutral con-

stituents in the TIS. Because these driving mechanisms show characteristic trends, the TIS too displays such trends, which essentially correspond to the climatology of the system. When it comes to smaller scale variabilities, the TIS could vary day to day and within a day, hour to hour, while displaying significant structures. These variabilities are essentially due to the external driving mechanisms which can be localized, spatially structured and temporally varying. As a consequence there could be significant time delays associated with certain TIS processes.

With this introduction, a brief outline will be provided for the ways and means by which the Thermosphere and the F-region of the ionosphere are mutually coupled with emphasis to low/equatorial latitudes followed by a discussion on the high-low latitude coupling and the middle-upper atmosphere coupling. Some discussion on certain aspects of the coupling are available in the literature[1] and the references cited therein and the significant contribution from the Indian scientific community had been comprehensively dealt by Agashe *et al*[2]. The present level of understanding of the interactive processes and their various manifestation into unique geophysical phenomena with specific reference to the equatorial region would be provided into the following sections.

Thermosphere-Ionosphere Coupling

The primary factors that affect the TIS are the neutral temperatures and winds. Whenever an additional energy is received by the atmosphere which is otherwise in equilibrium, the atmosphere gets heated up and this excess heating directly affects the density and composition in the region of deposition and also higher above. The result would be a net change in the $[O]/[N_2]$ ratio in the thermosphere which in turn decides the F-region electron densities. Differential heating of, like what one encounters in the day-night sides of the upper atmosphere, sets in large scale zonal winds effectively transporting energy and mass from the hot dayside to the cold nightside. The east-west zonal winds dragging the ionization along with it, cross with the north-south magnetic lines of force and generate the electric field which is the prime driving force for the consequent electrodynamical processes. On the other hand, the meridional winds which show a diurnal variability of being poleward during daytime, and equatorward during nighttime during geomagnetically quiet conditions, show a seasonal variability of being directed from the summer hemisphere to the winter hemisphere. The effect of poleward meridional wind on the ionosphere would be to push the F-layer down along the magnetic field lines and an equatorward wind would result in a net lifting up of the F-layer. During geomagnetically disturbed conditions since significant amount of energy deposition, overpowering the solar UV and EUV input, occurs at both the polar regions, there would be a convergent flow towards the equator redistributing the excess energy. This would cause an upliftment of the F-layer in both the hemispheres. On the other hand, any change in the plasma density distribution would modulate the neutral dynamical parameters, essentially due to the '**Ion-drag**' which refers to the resistance offered to the neutral winds by the ionospheric plasma which is confined to the geomagnetic field lines.

The coupled behaviour of the Thermosphere Ionosphere System (TIS) has been one of the important topics of research. Till recently there had been very little information available on this aspect from low latitudes. Systematic, coordinated measurements of thermospheric parameters viz., the neutral temperatures and neutral winds along with ionospheric parameters had been carried out from one of the low latitude stations, Mt. Abu (24.6° N, 72.7° E, geographic 18° N dip lat.) with a view to understand the mutual coupling under different geophysical conditions. One of the primary objectives had been to check the validity and applicability of Rishbeth's servo model. The above model[3,4] is one of the most elegant concepts highlighting the TIS behaviour and was originally formulated for mid latitudes. According to this model, in the absence of any external applied forcing, the height of the maximum electron density h_{max} would lie at a balance height determined by the diffusion and loss. During nighttime, in the absence of any fresh production of ionisation and in the absence of any applied forcings. The night stationary level 'h' would be located at a height where

$$\beta_m = \frac{k D_m \sin^2 I}{2H^2 (kac - 1)}, \qquad ...(1)$$

where β_m is the effective recombination coefficient, D_m is the plasma diffusion coefficient, H, the atomic oxygen scale height, I, the magnetic dip angle and k, a, c are constants, the former two referring to the layer shape factor and the ratio between the atomic and molecular species.

It could be seen that both β_m and D_m are neutral temperature dependent. It had been experimentally determined that a change of 100K in the neutral temperature would effect a change of 11 ± 4km in the balance height of the F-layer, over Mt. Abu/Ahmedabad (23.0° N, 72.6° E, 17° N dip lat.)[5]. These figures were arrived at based on the data when the meridional winds were close to zero and when the electric field effects were taken to be negligibly small. When one takes the meridional neutral wind (U_p — poleward positive) effects into account the servo equation takes a shape as[6-8].

$$-U_p \sin I \cos I = \frac{D_m \sin^2 I}{2H}\left[\exp\left[\frac{h_{max} - h_0}{H}\right] - \exp\left[\frac{-k(h_{max} - h_0)}{H}\right]\right] \qquad ...(2)$$

For moderate wind speeds not exceeding $100ms^{-1}$, the response could be treated as linear and the maximum effect in terms of ionospheric change would be experienced at a magnetic latitude of ~ 22.5° i.e. at a dip angle of 45°[9].

Spectroscopic measurements from Mt. Abu and independent ionospheric measurements from Ahmedabad were made use of in validating the applicability of the servo model to low latitudes. Excellent agreement between the estimated h_{max} and the measured h_{max} (Fig. 1*a*), during magnetically quiet periods had been shown[10]. It had also been found through case studies that the coupling remains intact even during magnetically disturbed periods[11] (Fig. 1*b*).

One of the important results from the coordinated measurements is that the neutral temperatures and the neutral winds have an independent control on the status of the F-region of the ionosphere at any instant. This has important consequences when one attempts to derive any one of the neutral atmospheric parameters from the observed variabilities in the F-region. A case in point is the use of F-layer movements during nighttimes and ascribe the same to the meridional winds[9,6,7] taking the model predicted temperatures to represent the thermal state and the distribution of the atmospheric species at that instant. However, it is fairly well accepted that the present day models do not represent the equatorial and low latitude regions (This aspect will be touched upon later). Therefore, unless one ascertains that the model and the actual measurements agree, the derived meridional winds on the basis of the above assumption would turn to be erroneous. These points are explicitly brought out by Gurubaran *et al*[8]. In the exercise of checking the applicability of servo model to low latitude regions, the measured neutral temperatures (T_n) had been taken as the exospheric temperature and the density distribution worked out following the formulation of MSIS-90 model[10], thus avoiding the said problems.

On the other hand, unlike Miller *et al*[9], Krishnamurthy *et al.*[12] have evolved an innovative method, wherein they have made use of the ionosonde data from two stations, one right over the dip equator, Thumba (8.3° N, 76.5° E, 0.35°N dip lat.) and the other, Sriharikota (13.3° N, 81° E, 5.35°N dip lat.) just located outside the equatorial electrojet for deriving the meridional winds. The latter has a finite magnetic dip angle of ~ 11° and therefore the F-layer movements would be controlled by the meridional winds as well, in addition to the electric fields, while the dip equatorial station is controlled only by the electric fields. The difference between these two locations has successfully been used to derive the meridional winds. It is very well known that the neutral temperatures do not vary significantly between these two, close by, stations and its contribution to the F-layer movement is automatically nullified. The rationale and the logic followed by Krishnamurthy *et al*[12] has been validated by the wind measurements using rocket released vapour clouds from SHAR and its comparison with the ionosonde derived winds[13].

From the background information presented above, it could well be appreciated that the thermosphere and the F-region of the ionosphere exist as a closely coupled system with the changes in the parameters of any one promptly getting reflected in the other. As a system, the TIS is coupled to the other region as well. Fig. 2 depicts the intricacies in the TIS and its possible linkages[14] to other regions.

Equatorial and Low Latitude Processes

The equatorial thermosphere-ionosphere system is replete with a variety of geophysical processes peculiar to this region. All these processes are an outcome of the complex web of interactive processes which include, chemical, electrodynamical and fluid dynamical ones. Some of the most important ones are the equatorial electrojet (EEJ), equatorial ionisation anomaly (EIA), equatorial spread-F (ESF), neutral anomaly (NA), equatorial temperature and wind anomaly (ETWA), equatorial spread-F (ESF) and midnight temperature maximum (MTM). The local time dependence of these phenomena are well represented in a clock diagram (Fig. 3) by Abdu[28]. In the following sections, a brief outline of the present understanding of the phenomena along with their interactive nature will be provided.

a) Equatorial Electrojet (EEJ)

The EEJ refers to the intense band of current flowing in the east-west direction over the magnetic equator centered around 106km. The latitudinal extent is usually taken as ~ 6° though there are indications for it to be variable. The EEJ is understood to be due to electrodynamical processes of a horizontally stratified ionosphere with anisotropic conductivities. The global scale dynamo action with the neutral zonal wind as the main driving force, manifests itself as a primary east-west electric field over the dip equator. This field crossing with the north-south geomagnetic field and also due to the differential motion imposed over the electrons and ions, i.e., the former getting influenced by the $\overline{E} \times \overline{B}$ forcing due to the electron collision frequencies being smaller than the gyrofrequency and the latter experiencing only the influence of the electric fields due to the ion neutral collision frequency being larger than the gyrofrequency, results in the generation of a vertical Hall polarization field. This Hall polarization field once again crossing with the east-west field is believed to be responsible for the generation of EEJ. The characteristic feature of the electrojet like, the intensity, height, structure, day to day variabilities, and latitudinal width have been extensively studied in the past using ground based and space-borne techniques. These have been reviewed by Agshe *et al.*[2]. Excellent electrojet models have been de-

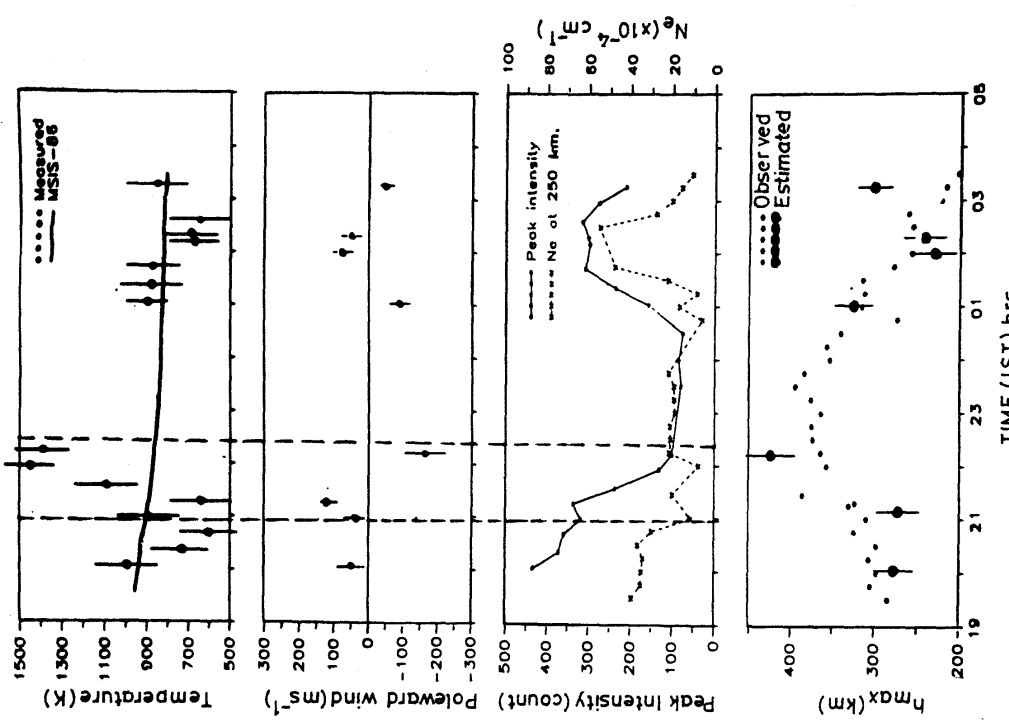

Fig. 1(*b*) Same as above for a moderately disturbed period. Relative airglow intensity variations are also provided in panel-3[11].

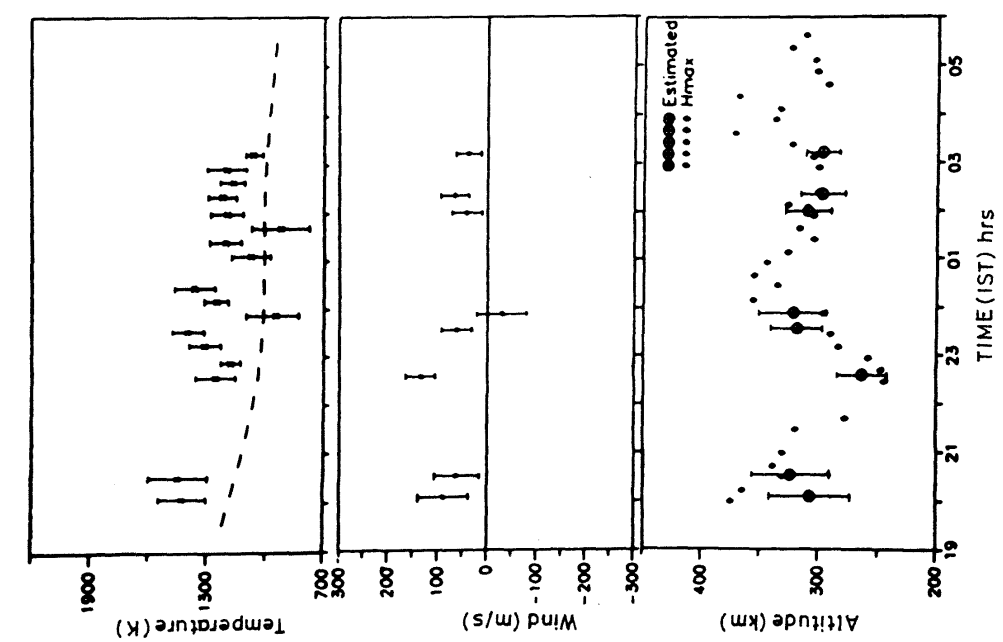

Fig. 1(*a*) Coupled behaviour of the low latitude thermosphere and the F-region of the ionosphere demonstrated through spectroscopically measured neutral temperatures (*top*) and winds (middle) alongwith the estimated h_{max} using Rishbeth's servomodel[3] and measured h_{max} using ionosondes[10] (*bottom*) during magnetically quiet times.

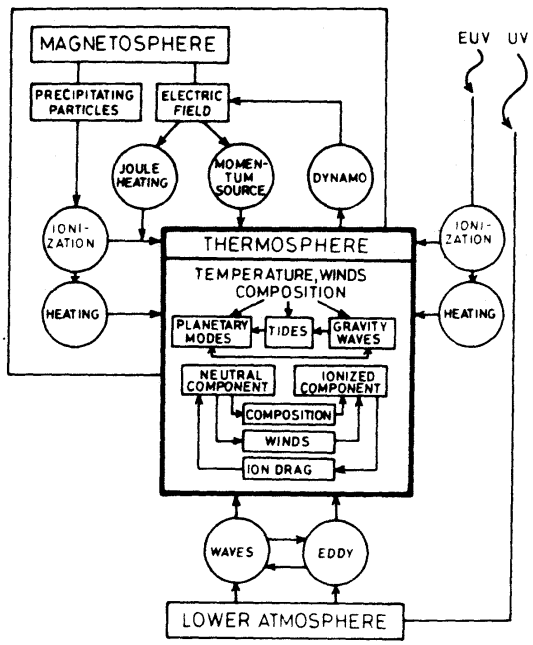

Fig 2 The mutually interacting thermosphere and the F-region of the ionosphere alongwith the various means of inter coupling with the magnetosphere above and the lower atmosphere below—schematic[14].

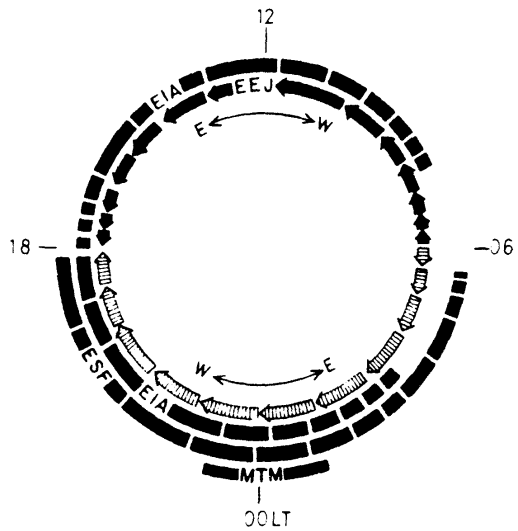

Fig. 3 Clock diagram representing the local time dependence of the unique geophysical processes[28].

veloped within the country and elsewhere which included the neutral wind effects on the electrojet and these are available in the literature[15-19]. One of the important aspects had been the prediction of vertical ion currents (Pedersen) by Untiedt[20] and demonstration of the importance of these currents in the generation of a deep valley in the plasma density profiles at ~ 120km during night time over the equator and significant enhancement in densities ~100km[21]. One of the unsolved problems with regard to the EEJ is the reason for the difference in the theoretically predicted altitude of maximum current (102km) and the actual location of the same (106km). One of the possibilities for this difference could be the unrealistic collision frequencies used in the model. By introducing a time varying additive term to the collision frequency, it is possible to explain the observed differences (B V Krishnamurthy - Personal Comm.). More detailed confirmation is called for by means of coordinated ground based and rocket experiments.

The other enigmatic aspect of the EEJ phenomenon is the counter electrojet (CEJ), when, during magnetically quiet periods, on certain occasions, during noontime, the EEJ might reverse its direction from eastward to westward for ~ 3*h* before recovering to its normal direction. The intensity and direction of the EEJ are usually inferred from the horizontal component of the ground level magnetic data. The differences in instantaneous value of the '*H*' component and the average nighttime value, from a location over the magnetic dip equator (ΔH_T) and another location away from the dip equator (ΔH_A) are taken and the differences in (ΔH_T) and (ΔH_A) is considered as a measure of the EEJ. One of the important results had been the disappearance of a particular type of sporadic-*E* layer, E_{sq}, during CEJ periods[22,23]. The enigmatic aspect of CEJ had been pertaining to its causative mechanism. There is no doubt that, it is the neutral dynamics that should be playing the deciding role but how exactly is what is being currently debated. Numerical simulations have revealed that upward vertical winds have the potential to reverse the current flow[24]. While there are evidences for distinctly different zonal winds on CEJ days with different shears in them[25] (Fig. 4). Meanwhile, Stenning[26] suggests that the CEJ may not after all be a localized phenomenon, and goes on to provide examples of global scale changes in the electric fields during CEJ. This opens up another fundamental question whether CEJ is a local phenomenon or a global one; or are there two types of CEJ's? Further work is needed to resolve these aspects. In addition, more observations are needed on the dynamo region tidal components and their variabilities from a global perspective.

In this context, two of the SCOSTEP sponsored programmes the PSMOS (Planetary Scale Mesopause Observing System) and the EPIC (Equatorial Processes Including Coupling) planned from 1998 onwards, are very relevant.

b) Electrojet During Disturbed Times

The geomagnetic disturbance related electric field perturbations fall in general into two types. The first type is the one which responds to the sudden change in the north-south B_z component of the inter-planetary magnetic field (IMF) to '**northward**'; the imposed additional zonal electric field is in phase opposition to the prevailing ones. On certain occasions, alongwith the sudden '**southward**' swing of the IMF B_z, transient disturbances, in phase with

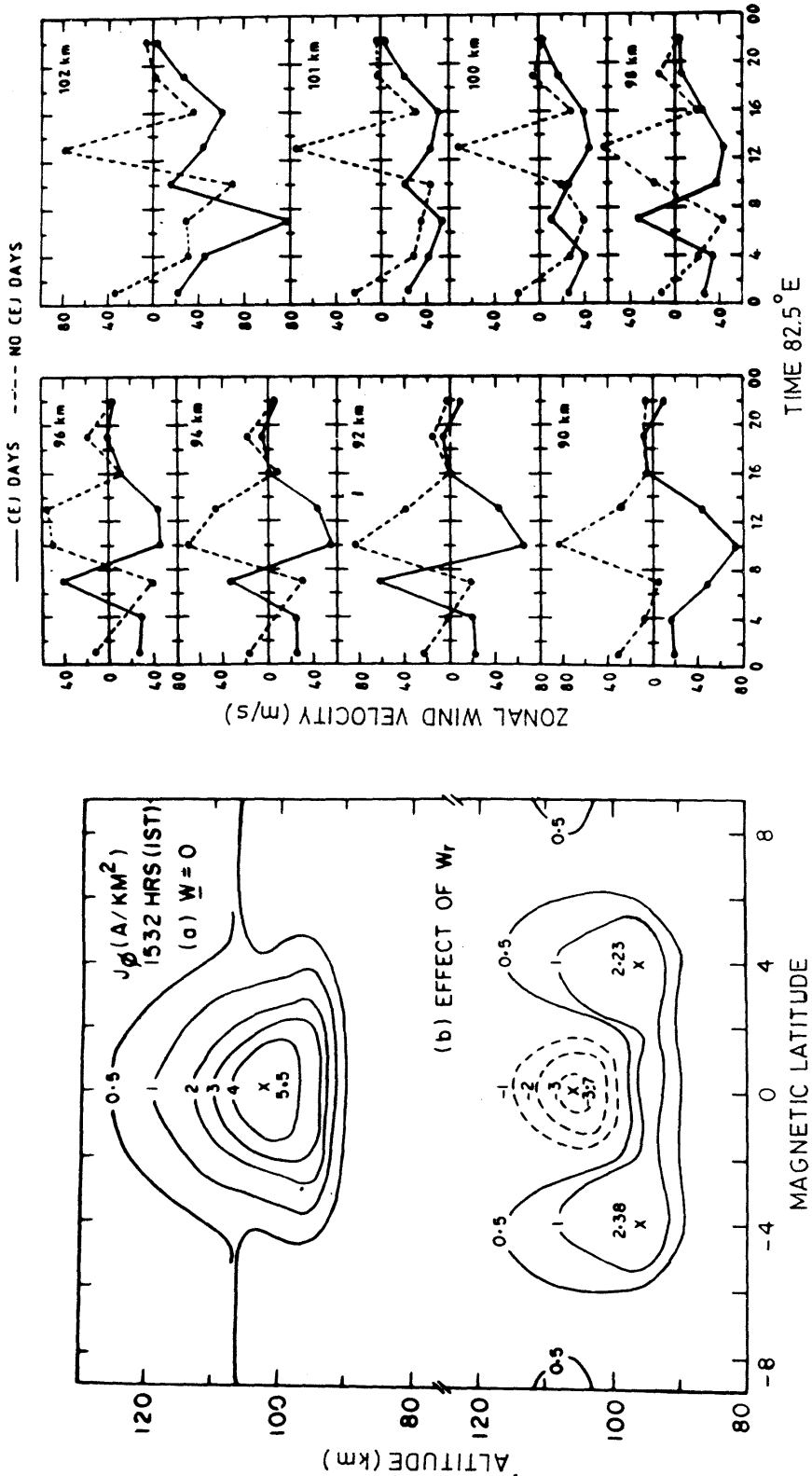

Fig. 4 Model calculations on the equatorial electrojet (left)- *(top)* - No winds *(bottom)* including vertical winds depicting the generation of counter electrojet (CEJ)[24]. (right) - Distinctly different shears in the zonal winds on CEJ days as compared to normal EJ days[25].

the quiet day field pattern have also been observed. These transient disturbances in the equatorial zonal electric field are believed to represent the effects of '**prompt penetration**' of high latitude electric fields into the equatorial ionospheres (Fig. 5*a* & *b*)[65,27].

The second type refers to the long lasting (several hours duration) and slowly varying part, which follows the onset of a geomagnetic storm, with long time delays (13-24h) and always opposing the quiet time fields (Fig. 6). These disturbances are believed to be due to the ionospheric disturbance dynamo i.e., due to the electric fields generated by the modification in the global thermospheric circulation caused by the storm time energy input over high latitudes. Fairly realistic models of penetration electric fields in the sub-auroral ionosphere associated with sudden changes in the magnetospheric convection have been developed by considering magnetosphere and the ionosphere as a coupled system and by paying due atten-

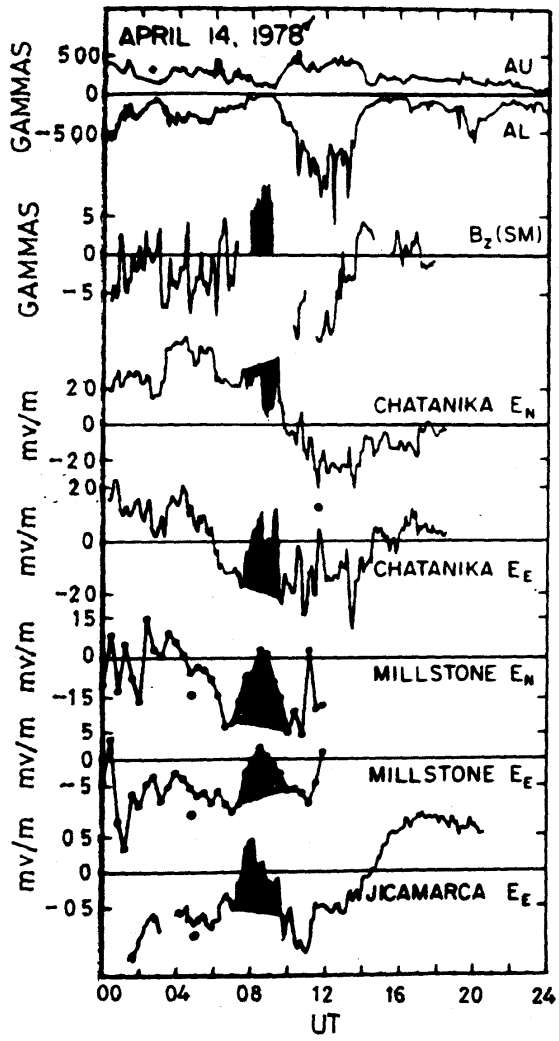

Fig. 5(*a*) Examples of 'prompt penetration' of high latitude electric fields to low/equatorial latitudes[67] from Jicamarca.

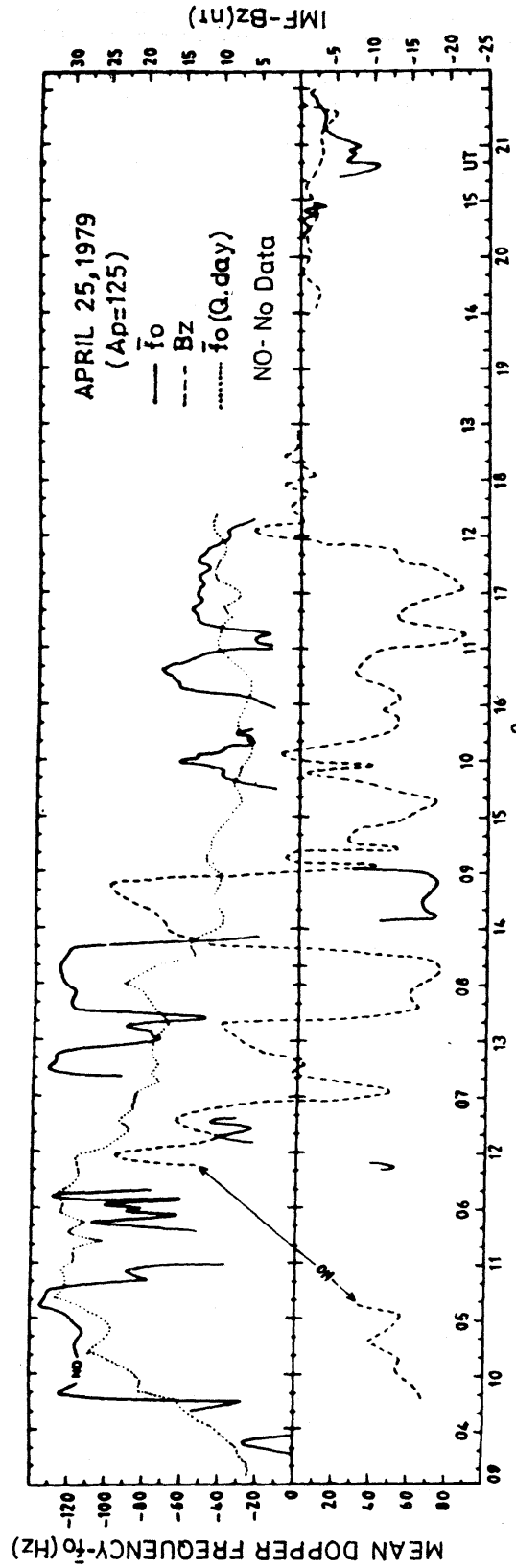

Fig. 5(*b*) Results from Thumba - temporal variation of the mean Doppler frequency of the VHF backscatter radar returns during a magnetic storm (continuous line) alongwith the IMF B_z(dashed line) and also the quiet time Doppler frequency variation (dotted line)[27].

tion to various physical processes operating therein. Though the global convection models predict the nature of the diurnal variation and their association with polar cap potential and also the latitudinal variation of the penetration electric fields fairly well, they cannot yet offer an explanation for the more sensitive response to decrease in the polar cap potential than to an increase in the same. Also the long persistence in the zonal electric field associated with the magnetospheric convection in addition to the mutually exclusive transient electric fields associated either with an increase or decrease in the magnetospheric convection, but not both, needs to be understood[28]. All the above, indicate the need for a concerted theoretical study to explain the physical mechanism that essentially controls the penetration of high latitude electric fields to the dip equator under storm and substorm conditions.

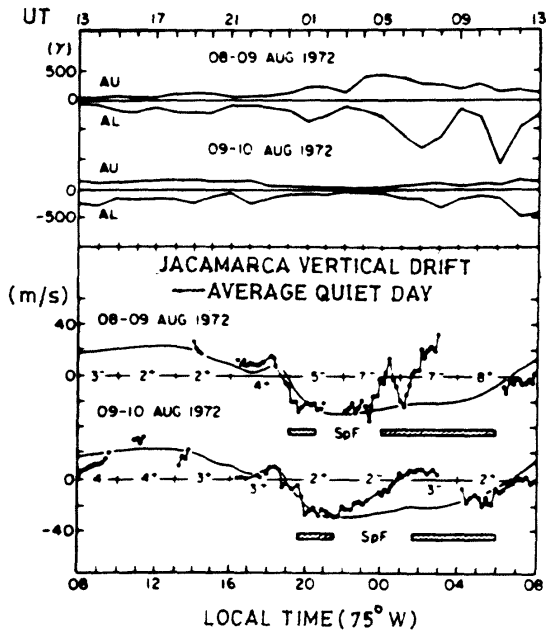

Fig. 6 Slowly varying disturbance dynamo electric fields with long time delays (13-24h) associated with a geomagnetic storm[67].

c) *The Equatorial Ionization Anomaly (EIA)*

The EIA is one of the most prominent equatorial ionospheric/thermospheric processes and it refers to the development of a double humped structure in the latitudinal profile of the F-region plasma densities during daytime with the crests located at ± 15–20° dip latitudes and the trough situated over the dip equator. This phenomenon has been fairly well investigated using ionosondes and airglow photometers both from ground and satellite-borne, and total electron content measurements (TEC) using beacon transmitters in the orbiting and geostationary satellites[29]. It is fairly well understood that, it is the plasma transport controlled by the electrodynamical processes assisted by the neutral dynamics that redistributes the same resulting in the EIA. During night hours, the reverse happens with the plasma being drawn back towards the equator[30-32]. There are still several enigmatic aspects left out with regard to the EIA, though the gross features are well understood. One of the puzzling aspects being the longitudinal variability exhibited by this phenomenon. One might observe strong EIA in one longitudinal zone but it might be totally absent in a zone separated by just 30°[33]. Global coverage by the DE-2 satellite also revealed this aspect more dramatically (Fig. 7). These results make the predication of EIA very difficult. Not limiting to this, even the solar cycle dependence of EIA and also its behaviour during magnetically disturbed periods still remain topics of active research[34].

d) *EIA - During Disturbed Periods*

The EIA responds sensitively to the disturbance electric fields and winds. It could either get enhanced or inhibited depending upon the nature of the disturbance electric fields. These fields are in general of two types; the first one being the penetration electric fields as mentioned above which involve hydromagnetic wave propagation and ionospheric currents[35-37] or substorm current system, and shielding by the inner magnetosphere associated with the changes in the IMF polarity[38-40]. The second type is due to the changes in the general circulation due to the significant energy deposition at polar latitudes, which sets in a disturbance dynamo field. Further, the effect of meridional winds, as mentioned earlier, would be to lift up or push down the ionization along the field lines depending upon their polarity, whether it is equatorward or poleward.

Transequatorial wind would cause an asymmetry in the EIA crests. The degree of the asymmetry being dependent on the two competing forces, namely, the magnitude of the wind the zonal electric field. However, these effects are prominently felt only in the case of a slowly evolving plasma fountain. In the case of transient events like the post sunset enhancement in the electric field or during transient penetration of electric fields during disturbances, the effect of transequatorial winds would not alter/or create any asymmetry in the evolution of the EIA. Simulation studies do support the above idea[41]. However, quantitative estimate of the effect of disturbance electric field in the evolutionary characteristics of the EIA remains to be made yet. Some of the important results obtained in the recent years are the expansion of the latitudinal region contributing to the fountain, sometimes extending to even lower mid latitudes, in response to a transient disturbance electric field. When such an explanation occurs in the dusk sector, a similar expansion has been noticed in the predawn sector, eventually resulting in the inhibition of EIA development. On the other hand, the effect of the disturbance dynamo

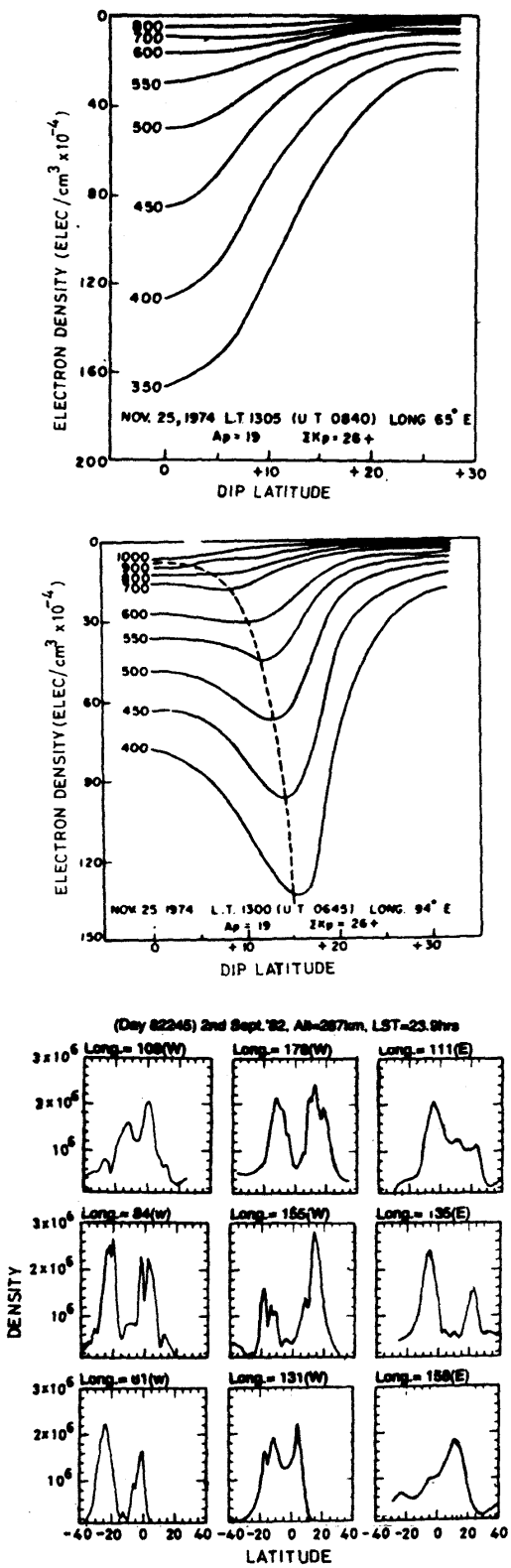

Fig. 7 (*top*) - The presence and absence of equatorial ionization anomaly within a longitude separation of 30 deg., based on topside sounder data[33].
(*bottom*) - The dramatic longitudinal differences in the EIA as detected by DE-2 satellite[11].

electric field on the EIA would be to inhibit its formation during day and post sunset times and also to enhance its development during night hours. The picture with regard to the response of the EIA during disturbed periods is quite complex and it has just started emerging. More detailed experimental and theoretical efforts are needed for a thorough understanding of the same. All these aspects are comprehensively reviewed by Abdu[28].

e) The Equatorial Temperature and Wind Anomaly

As mentioned during the discussion on the coupled beha-viour of the thermosphere and the ionosphere, the neutral wind acts as the main driver of the global scale dynamo which in turn sets in phenomena like the EEJ and EIA. On the other hand, the neutral flow itself is affected by the ionosphere in two ways. At the dip equator when the F-layer is lifted-up due to the $\overline{E} \times \overline{B}$ plasma drift, it would deplete the region lower below, thus reducing the ion drag. This would permit relative acceleration of the neutral winds over the dip equator[42-43]. The so called F-region dynamo, (to be discussed later) analogous to the E-region dynamo, generates vertical polarization fields which in turn would drive the plasma along with the neutral wind[44]. Once there is little relative motion between the ions and neutrals, the ion drag is further reduced. During daytime conditions the F-region dynamo effects are shorted out by the loading of the system by the field line connected E-region conductivities and the ion drag effects would be significant. In fact, first it was shown using OGOVI satellite data, that the latitudinal distribution of neutral densities show some sort of a geomagnetic control with two crests of densities colocated with the EIA crests and a trough over the dip equator[45]. It was suggested by them that the enhanced drag offered by the EIA crests to the neutral zonal flow from the hot dayside to the cold nightside would result in the accumulation of neutrals at the crest locations. If that be the case, one would expect to see enhanced neutral temperature at the crest location simultaneously with reduced zonal winds. The first experimental evidence to this effect was obtained by Raghavarao *et al.*[46-47] using DE-2 satellite data. The phenomenon referred to as the Equatorial Temperature and Wind Anomaly (ETWA) is one of the classical examples of the interacting thermosphere-ionosphere system. Simultaneous measurements of plasma densities, neutral zonal winds, and neutral temperature along a given longitude revealed clearly the zonal wind velocity to be maximum at the dip equator colocated with the trough in the plasma densities and a minimum in the zonal winds was seen at the crests of the EIA. Also the neutral temperature enhancements were colocated with the EIA crest and zonal wind minimum. There was a temperature minimum at the trough (Fig. 8*a*). In addition to the above, vertical winds were detected presumably associated with ETWA[47]. The

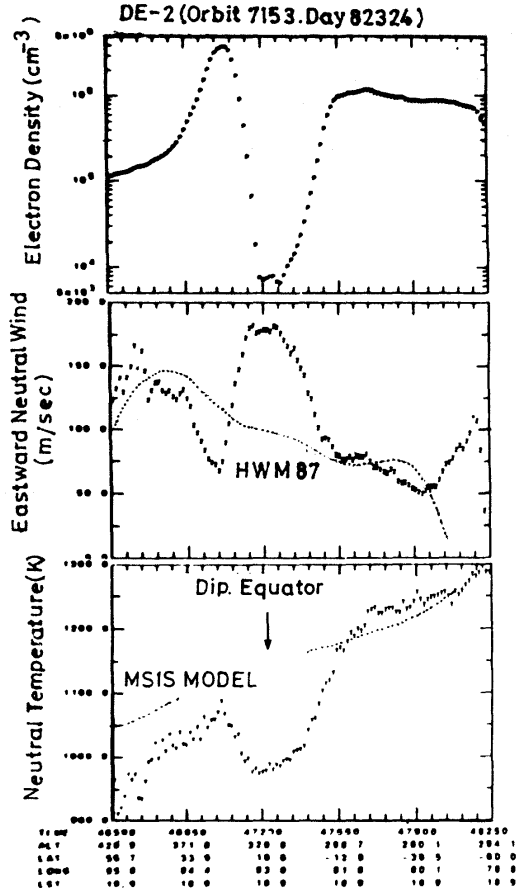

Fig. 8(*a*) The phenomenon of Equatorial Temperature and Wind Anomaly (ETWA). The decelaration of zonal wind (*middle*) at the crest location (*top*) and the enhancement of neutral temperature (*bottom*) as seen in the coordinated measurements of DE-2[46].

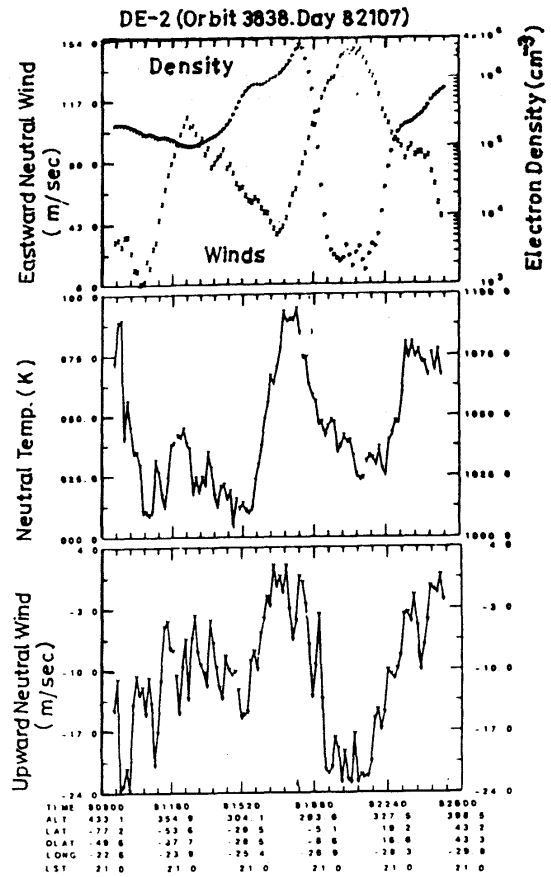

Fig. 8(*b*)

Fig. 8(*b*) (*Right Top*) The presence of ETWA and the associated latitudinal variation of vertical winds. Upward winds over the crest and downward winds at the trough locations[47]

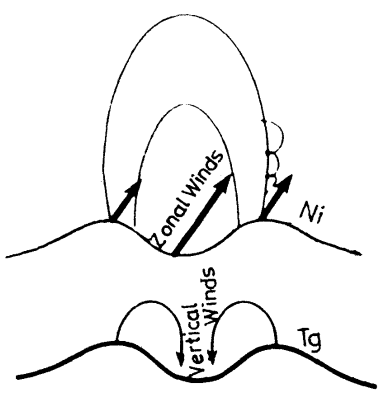

Fig. 8(*c*) The proposed mechanism of meridional circulation with upward winds at the crest and downward winds at the trough latitudes[47].

winds were directed upward at the crest location and downward at the trough leading to the suggestion that these could after all be a part of the circulation cell with equatorial winds in the upper and poleward winds in the lower thermosphere (Fig. 8b). The magnitude of the vertical winds were directly related to the strength of ETWA. These results have very important significance with regard to the phenomenon of equatorial spread-F which will be discussed later.

Coming back to ETWA, the exact causative mechanism had been an active topic of research. Whether it is '**ion drag**' or some other mechanism or both are responsible for its creation has been the basic question. Raghavarao *et al.*[48] conducted a detailed study on the diurnal variability of ETWA both in terms of neutral temperatures and neutral winds. They had considered the difference in neutral temperatures (ΔT) between the crest and the trough locations and so also in the case of winds (ΔZ). The magnitude of (ΔZ) was shown to be proportional to the zonal wind Z at the equator and usually at 50% of the latter's magnitude. On the other hand, the magnitude of ΔT was dependent on both the zonal wind and the strength of *EIA*. They had shown that the ΔT became minimum at local times when the zonal wind (ΔZ) was close to zero, indicating that the magnitude of the zonal wind irrespective of the direction is one of the important

parameters. The ETWA was shown to be the strongest around 1900-2000 LST when usually the EIA and the zonal winds were at their maximum. The development of ETWA during daytime is strictly linked to the EIA, as the zonal winds usually attain their maximum earlier and stay so through out the day (Fig. 9). This led them to state that the ion drag must be playing a crucial role. On the other hand, Fuller-Rowell *et al.*[49], in an independent exercise, suggested that the kinetic energy getting converted into thermal energy due to ion drag may not be the appropriate mechanism. They also showed that the mechanism of horizontal transport appears to work in the wrong sense. It

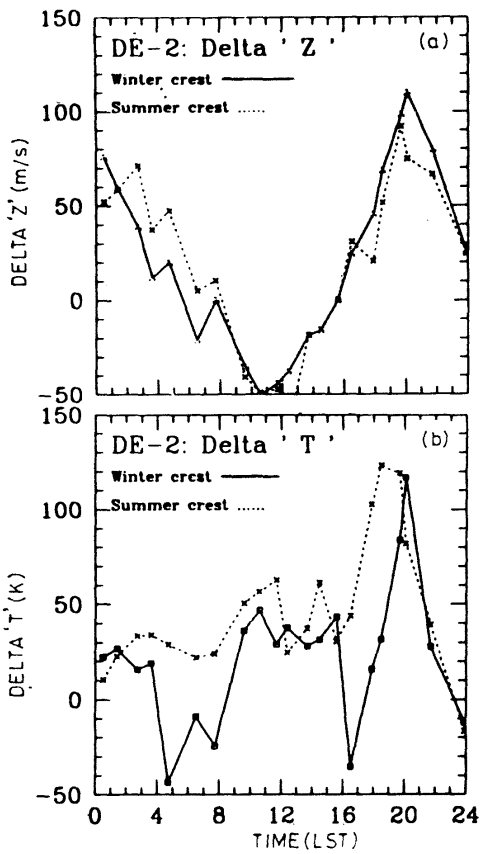

Fig. 9 Local time variation of ETWA temperatures (*top*) and ETWA zonal winds[48].

was also made clear[46,49] that adiabatic cooling and heating originally suggested by Anderson and Roble[42] would produce a temperature structure that would require upwelling with cooling and downwelling with heating, while the measurements reveal the contrary[47]. Since the DE-2 measurements call for a source of heat at the EIA crests where winds are damped, Fuller-Rowell suggested that chemical heating could be responsible for ETWA. The large fraction of the ionization energy from recombination could be converted to heating of the neutral gas. At the peak of the EIA crests, the two stage recombination process of O^+ ions is exothermic and is controlled by the rate of the reaction

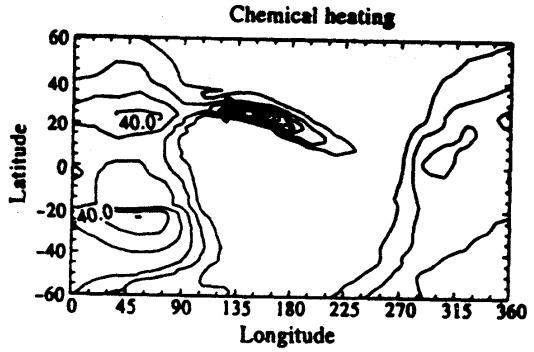

Fig. 10 (*left*) - Two dimensional simulation of ETWA based on ion chemical scheme involving exothermic reactions[49].

with N_2 and O_2. The combined heating rate at 300 km for an exospheric temperature of 1000 K was estimated to be ~ 200 K/h[49]. Fig. 10 depicts the ion chemical schemes suggesting that chemical heating could be a possible candidate for ETWA. The chemical heating proposed by Fuller-Rowell *et al.*[49] occurs irrespective of the time of the day and is dependent on the constituent densities only. However, the magnitude of the estimated heating is not always commensurate with what has been observed by DE-2.

More recent, detailed, studies using the DE-2 data enable the quantification of chemical and ion drag contribution to ETWA. During nighttimes, whatever ETWA had been detected by DE-2 could straightaway be ascribed to the chemical heating, as the ion drag-effects would be negligible due to the F-region dynamo action, and the relative velocities between ion and the neutrals being negligibly small. The estimates revealed ~ 30% contribution due to chemical heating while the remaining to be related to the ion drag effects[11], thus offering a viable explanation for the occurrence of ETWA.

f) The Midnight Temperature Maximum (MTM)

The local maximum in neutral temperature around midnight hours over low/equatorial latitudes is referred to as the Midnight Temperature Maximum (MTM). The first ground based observations of certain manifestation of the MTM were made by Greenspan[50] from equatorial latitudes, and by Nelson and Cogger[51] from Arecibo, using OI 630.0nm photometers. The red line intensities registered enhancements, the local time of, occurrence of which shifted systematically to later times as one moved away from the equator. Behnke and Harper[52] later explained the downward movement of F-layer due to the MTM associated pressure bulge over the equator. Jicamarca radar results on electron temperatures presumably linked to MTM, revealed that the MTM appeared, at local midnight during local winter, and at 2100-2200 LT during local summer (Fig. 11*a*). The first *in situ* measurements of MTM

were made by Spencer *et al.*[53] using the Neutral Atmosphere Experiment (NATE) in the AE satellite. The simultaneous measurement of meridional winds confirmed the polarity reversal in them during MTM. Seasonally, the MTM is known to occur earlier and stronger in local summer and symmetrically during equinox. However, the general pattern had been an MTM which is centered on the geographic equator with two additional maxima (Fig. 11*a*). A comprehensive review on MTM is available in the literature[54].

From the Indian longitudes Renganathrao and Hanumanth Sastri[55] studied the characteristic features of the MTM from Kavalur (12.5° N dip lat. 4.25° N) using ground based high resolution spectrometry of the thermospheric OI 630.0nm airglow line. They had observed the occurrence to be atleast one hour after midnight during local winter and just before midnight during vernal equinox, in broad agreement with the Jicamarca radar results (Fig. 11*b*). As for the amplitude of the MTM is concerned, it had been shown to be larger in the Indian logitude, than in the Americal longitude[56]. Sastri *et al.*[57] also provided direct experimental evidence by coordinated optical and ionosonde measurements for the significant control the MTM and the associated thermospheric dynamics have on the low latitude F-region (Fig. 12) thus providing further confirmation to the inference made by Behnke and Harper[52].

A plausible explanation for the MTM was first offered by Mayr *et al.*[58] which was later supplemented by Herraro *et al.*[59]. The MTM was ascribed to ion-neutral momentum coupling processes. The diurnal wind variations when coupled to the diurnal ion density variations, wavelike oscillations would result in an MTM. In other words, nonlinear interaction of the higher tidal modes of the thermospheric winds driven by solar *in situ* forcing and the modulation of the electron density by the production of the F-region ionization would be responsible for the MTM (Fig. 13*a*).

However, simulation studies using the NCAR-TGCM model could not reproduce the MTM inspite of including realistic solar forcing and ion-neutral momentum coupling in it. But once the effects of waves originating from the lower atmosphere were included the MTM could successfully be reproduced[60] (Fig. 13*b*). Through detailed simulation studies using the TIEGCM model, it had been shown that the upward propagating semidiurnal tides might really hold the key for this phenomenon. The major difference between the above suggestion and that from Mayr *et al.*[58] being that, in the case of the latter, only contributions from symmetric diurnal modes with identical horizontal and vertical extent were included, while the current understanding is, that, the symmetric mode contributions for the upward propagating waves are negligible[61-63].

Inspite of the successful simulation by the TIEGCM, still there are certain limitations as the low latitude ionosphere is not realistically simulated by the model. It could be seen in the failure of the TIEGCM model in reproducing the post-sunset F-region upliftment[64]. Notwithstanding this limitation, it could be considered that, that the day-to-day variability could as well be due to the variability in the upward propagating tides, while the seasonal variability could be due to the interaction between the (2,2) and (2,3) modes as they reinforce each other in summer and offset in winter. More detailed investigations are called for with a realistic low latitude ionosphere serving as input to the model.

g) Equatorial Spread-F (ESF)

The phenomenon of equatorial spread-F (ESF) refers to one of the turbulent conditions of the nighttime equatorial ionosphere, wherein plasma density irregularities, the scale sizes of which range from a few centimeters to several hundred kilometers, get generated under favourable conditions, mainly due to a hierarchy of plasma instabilities operating therein. By far, the ESF is the most complex and enigmatic plasma process and it manifests itself in a variety of ways. For example, it is seen as 'scattered echoes' in ground based ionosondes, 'plumes' in the VHF-radars, 'airglow intensity bite-outs' in the optical techniques, 'bubbles' in the *in situ* satellite measurements and, VHF and UHF 'scintillations' in the ground based receivers, which receive the satellite beacon signals. The Rayleigh-Taylor instability is accepted to be the primary agency which destabilises the equatorial F-region making the situation conducive for a hierarchy of instabilities to operate. During post sunset hours over the magnetic equator, due to the F-region dynamo becoming active, the F-layer gets lifted to great heights and a steep density gradient in the bottomside gets developed due to the combined action of the uplifting and the chemical recombination in the E and F layers. The situation is analogous to a heavier fluid over a lighter fluid i.e., the hydrodynamic Rayleigh-Taylor instability[65,66]. Onset of the instability results in the upwelling of F-region of low density bottomside plasma, often to even 1000km and beyond, over the equator. The depletions are field aligned and therefore map along the entire magnetic flux tube to even beyond ±15° in latitude. In the zonal direction it may typically extend around 100-200km and drift towards east with a velocity of 50-150 ms^{-1}. On the average, the density depletions could be anywhere between 1-4 orders of magnitude. The walls of the depletions, where one encounters the steepest of the gradients, serve as the seat for the smaller scale density structures[67].

There is a stiong longitudinal dependence in the seasonal occurrence pattern of ESF. In the Atlantic region its occurrence is most favoured during northern winter, in

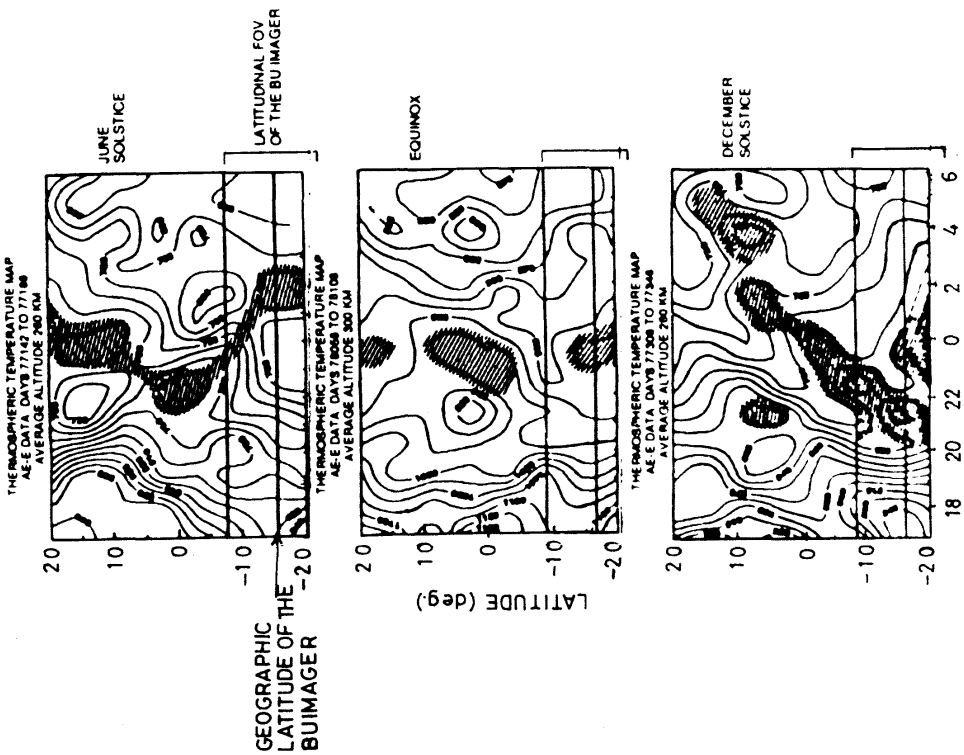

Fig. 11(*a*) The local time variation of the MTM during different season based on NATE experiment in the AE satellite[54]

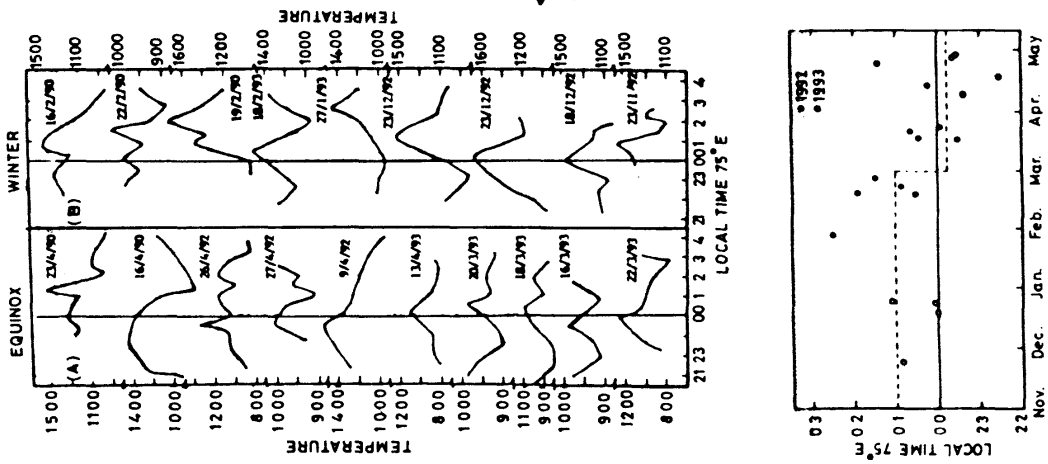

Fig. 11(*b*) Spectroscopic measurements of the MTM over Indian longitudes depicting the high degree of variability of the phenomenon both day to day and seasonal[55]

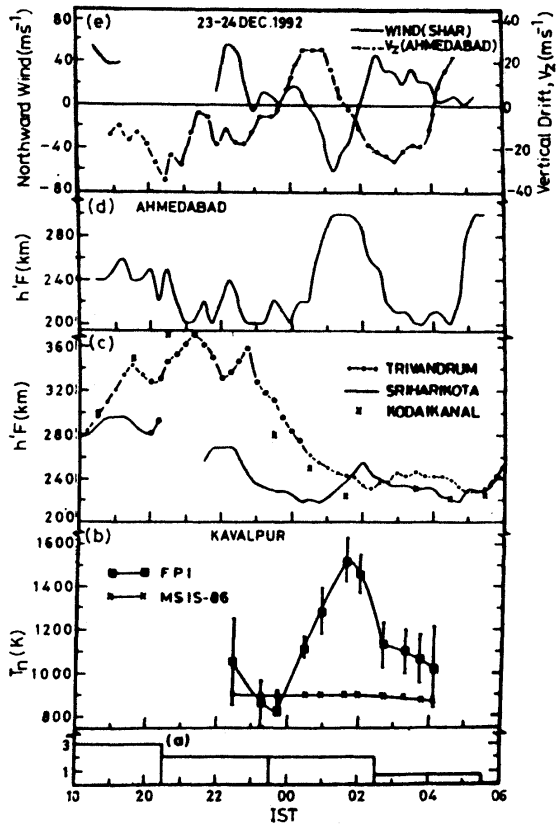

Fig. 12 Results from coordinated measurements depicting the large scale thermospheric dynamics induced by MTM. Corresponding response of the F-layer over low latitude station are depicted[57].

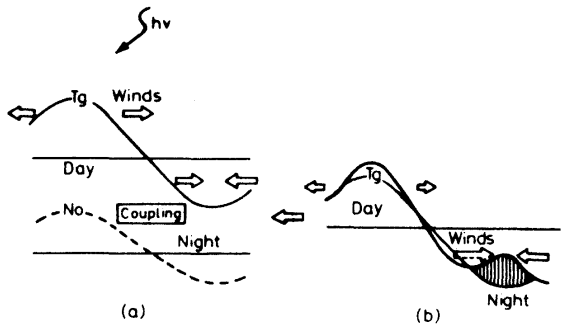

Fig. 13(a) Schematic representation of the nonlinear interaction between the tidal modes of thermospheric winds modulated by the F-region electron density variation[58].

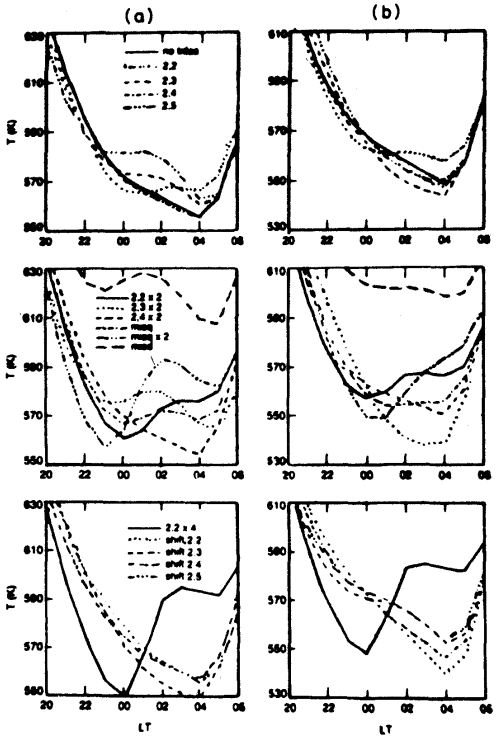

Fig. 13*(b)* Model simulation of nighttime neutral temperatures near 300km for September solar minimum conditions at *(a)* 17.5° S and *(b)* 17.5° N for different amplitudes and phases of the 2.2, 2.3, 2.4 and 2.5 tidal components[60].

the pacific region during northern summer and the South American and Asian zones during equinoctial periods[68-69, 71]. Maruyama and Matuura[68] attempted to explain the behaviour during solstices based on the meridional winds causing redistribution of ionisation i.e., when the EIA peaks are symmetric, ESF occurs and when they are asymmetric, presumably due to meridional winds, ESF gets inhibited. On the other hand, Tsunoda[69] explained the equinoctial maxima to be determined by the magnetic declination and geographic latitude of the magnetic equator i.e., in other words, based on the alignment of the solar terminator with the geomagnetic flux tubes, which results in enhanced polarization field and consequent plasma drifts. Both the above mechanisms have their own limitation, as in a given season and solar epoch and under seemingly identical ionospheric conditions ESF might occur on one day and might be totally absent on another, thus making the day to day variability into an enigmatic problem[70-71].

The two approaches presently being contemplated are i) the F-region during post sunset period is delicately balanced and an initial perturbation under favourable conditions could destabilise the same resulting in ESF and ii) everyday by default ESF should occur and an inhibiting agency controls the evolution of the same.

One of the prerequisites of ESF is the lifting up of the equatorial F-region to heights beyond 350-400km by the electric field generated due to the F-region dynamo[72-74]. During daytime conditions because of the presence of the E region, which is connected to the F-region by the highly conducting geomagnetic field lines, the F-region dynamo fields get shorted out and the E-region effectively controls the physics. The small daytime vertical electric fields in the F-region is presumably the meridional E-region electric fields mapped up along the field lines. In the post sunset period, however, the vertical field is enhanced due to the local F-layer dynamo during all epochs and seasons except during solar minimum periods. Heelis *et al.*[74] successfully predicted the post sunset effects by including horizontal conductivity gradients in addition to the well-known vertical gradients. Near a sharp east-west gradient as one encounters during sunset, an enhanced zonal electric field gets established in order to keep $V.J = 0$ (Fig. 14*a*).

In another simulation, Farley *et al.*[75] retained only the F-region electrodynamics and suppressed the E-region dynamo and imposed a uniform wind field. The shorting effect of the E-region was demonstrated during daytime and enhancement seen at both the terminators. Fig. 14*b* conceptually offers an explanation to the F-region dynamo. When the wind blows across the terminator, it generates a vertically downward electric field substantially larger in the nightside as compared to the dayside. This field when mapped to the E-region off the equator would drive a westward Hall current and results in a net accumulation of negative charges at the terminator creating a localized zonal E_Φ perturbation. This field when mapped to the F-region, crosses with the N-S magnetic field and results in the post sunset uplifting of the F-layer.

The third mechanism proposed by Haerendal and Eccles[76] tries to account for the unaccounted surge in electric field by incorporating the electrojet effects during sunset hours. It is envisaged that in order to maintain current continuity, there would be a vertical current flow at the sunset terminator which would result in an enhancement of the postsunset polarzation electric field. Though presently, the first mechanism is more favoured[77], further experimental confirmation is needed. It is an important element as post suset uplifting is essential for ESF and a complete understanding is a must in order to be able to predict its occurrence.

Generally, it is believed that gravity waves provide the necessary seed perturbation which have been detected from the height modulation of the F-region[78,79]. Satellite measurements (SANMARCO-D) revealed that equatorial plasma depletions are associated with eastward electric fields ranging from 3-30 mVm^{-1} corresponding to upward velocities[80] of 100-1000 ms^{-1} and on rare occasions even bubbles with supersonic velocities have been recorded[81].

Several attempts have been made to develop linear theories and nonlinear numerical simulation in order to understand the complexities of the phenomenon[65,82]. A review of these aspects has been given by Ossakow[66]. Sekar and Raghavarao[83] derived an expression for the growth rate of the generalized R-T instability including the effects of neutral winds and demonstrated that vertically downward winds could play a crucial role in enhancing the growth rate of the R-T instability (Fig. 15). Haerendal[65] highlighted the need for considering field line integrated ionospheric quantities. These quantities along with realistic atmospheric and ionospheric density models were substituted in the growth rate expression[84]. The growth rate being positive implied occurrence and negative implied nonoccurrence of ESF. A new derivation of the linear R-T growth rates including the effects of ionospheric electric fields, neutral winds, a finite E-region and horizontal ionospheric gradients in density and conductivity has been made by Sultan[84]. The important result of the above attempt is that the time/altitude domains of positive growth rate coincided with observations on a larger time frame (Fig. 16). A detailed treatment of this new linear formulation is available in the above referred literature.

However, the evolution of the ESF phenomenon is nonlinear and therefore only nonlinear numerical simulation could give a realistic picture on its evolution[85-88]. Very important results highlighting the role of neutral dynamics in the triggering and evolution of ESF demonstrating that vertically downward winds could enhance the growth rate of plasma instability has been obtained. Further, the threshold limit for the initial perturbation ampli-

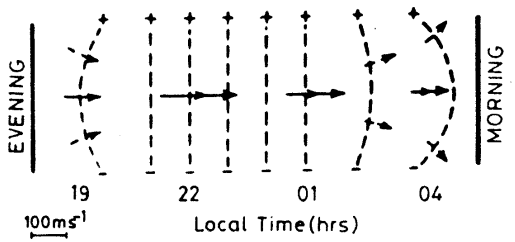

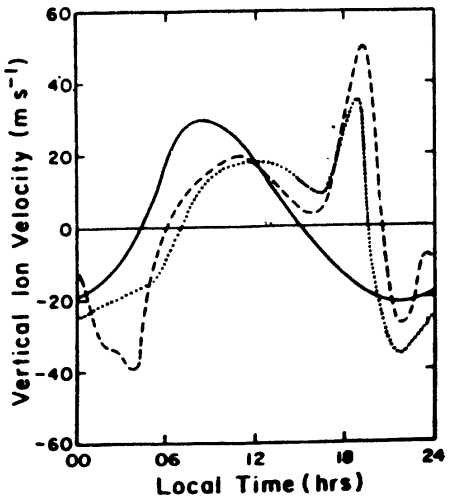

Fig. 14*(a)* (*top*) - The mechanism for the surge in the sunset terminator in the F-region dynamo based on the curl freeness of electric fields[72]. (*bottom*) - Successful prediction by Heelis *et al.* by including the horizontal conductivity gradients in addition to the vertical gradients[74]

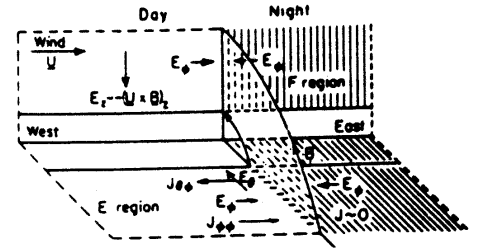

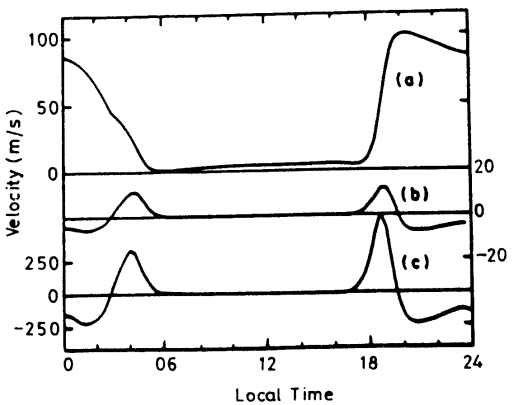

Fig. 14*(b)* (*top*) - Schematic representation of the electrodynamic coupling between the E and F regions resulting in the surge in the F-region dynamo[75]
(*bottom*) - The shorting effect of the E-region during daytime and this effect tapering off at the terminator resulting in the post-sunset uplifting of the F-region based on the above mechanism[75].

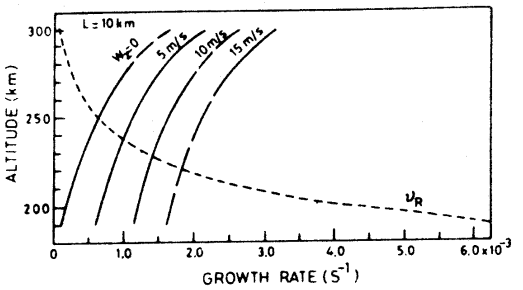

Fig. 15 A comparative study between the role of gravity and the vertical winds on the triggering and sustaining the equatorial spread-F, by linear theory. The larger the wind magnitude, lesser is the altitude where the instability could get triggered[83]

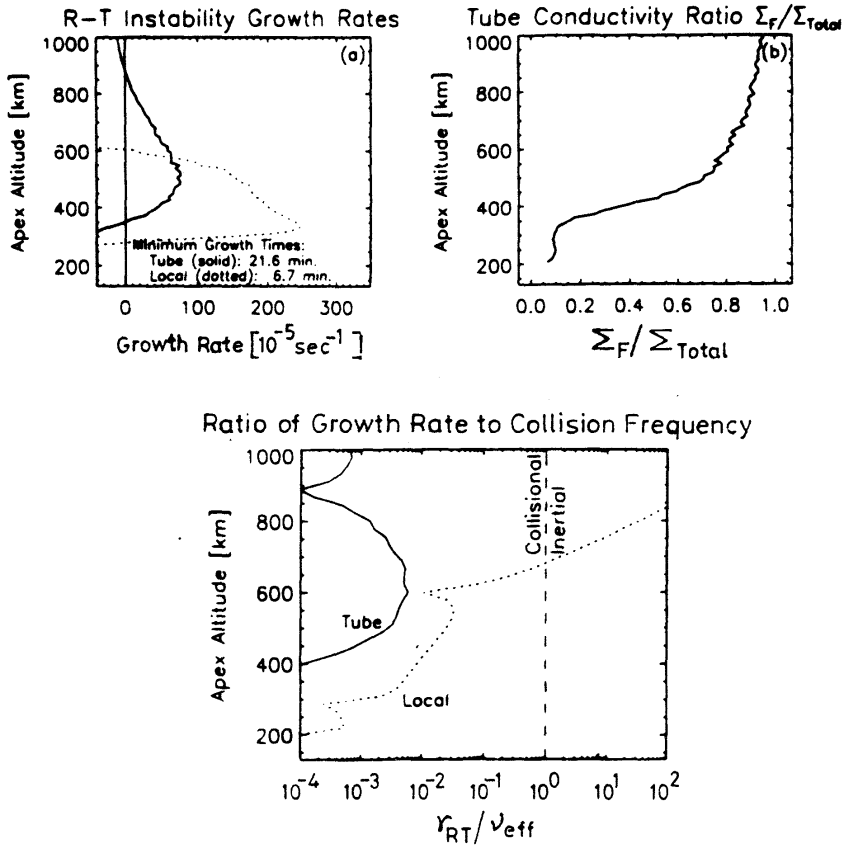

Fig. 16 Observed and estimated growth rates of the ESF, the latter having been done by taking into account the electric fields, neutral winds, a finite E-region and horizontal ionospheric gradients and conductivity[84].

tude was shown to be an order of magnitude less and only 0.5% under favourable conditions when all the other destabilising factors like the electric field, neutral winds (both zonal and vertical) are in phase and favour the instability[89]. The role of topside electron density gradient in the evolution of a plasma bubble was highlighted explaining the different manifestation of a bubble viz. mushroom or pillar like structure[90] and also the role of fringing fields in the generation of density irregularities in the bottomside F-region where the conditions including the plasma density gradient are otherwise not conducive for any instability[91] have been obtained, through nonlinear numerical simulation techniques (Fig. 17).

Laakso *et al.*[93] based on vector electric field and plasma density measurements using San Marco D satellite, revealed the complexities in the bubble structure and its evolution. Examples of updrafting bubbles (with positive E_y enhancement with an eastward tilt) and downdrafting bubble have been shown by them, though the latter is not very common (Fig. 18). In the example depicted above within the depleted region the downward drift spaced had been of 80-130 ms^{-1}, faster than the ambient plasma. Patra *et al.*[94] have provided examples of irregularity structures moving downwards as seen from the Indian MST radar, at Gadanki, Tirupati (13.5° N, 79.2° E, dip lat. 6.3° N). They had suggested that the above event could be an example for the downdrafting of a plasma bubble as seen by a VHF coherent radar. Sekar[92] through nonlinear simulation studies demonstrated that it may not be that simple an explanation, as the reversal in polarity of the electric field could at the most inhibit the evolution of a bubble and stabilize the F-region and never it could make a depleted structure move downwards along the gravitational force. As suggested by him the irregularity structures detected by the radar could as well be a region of enhanced densities which usually flank a depletion on either side close to the wall of the bubble making the distinction extremely difficult. The point is under heated debate and more intense studies, both observational and theoretical are needed to unravel the enigma.

Once, both the neutral dynamical and electrodynamical parameters independently control the evolution of ESF, it is but natural that this phenomenon would be affected during geomagnetically disturbed periods as well. The analogy is similar to the occurrence of EIA. An increase in the evening transequatorial wind/or a decrease in zonal wind arising from storm induced disturbance

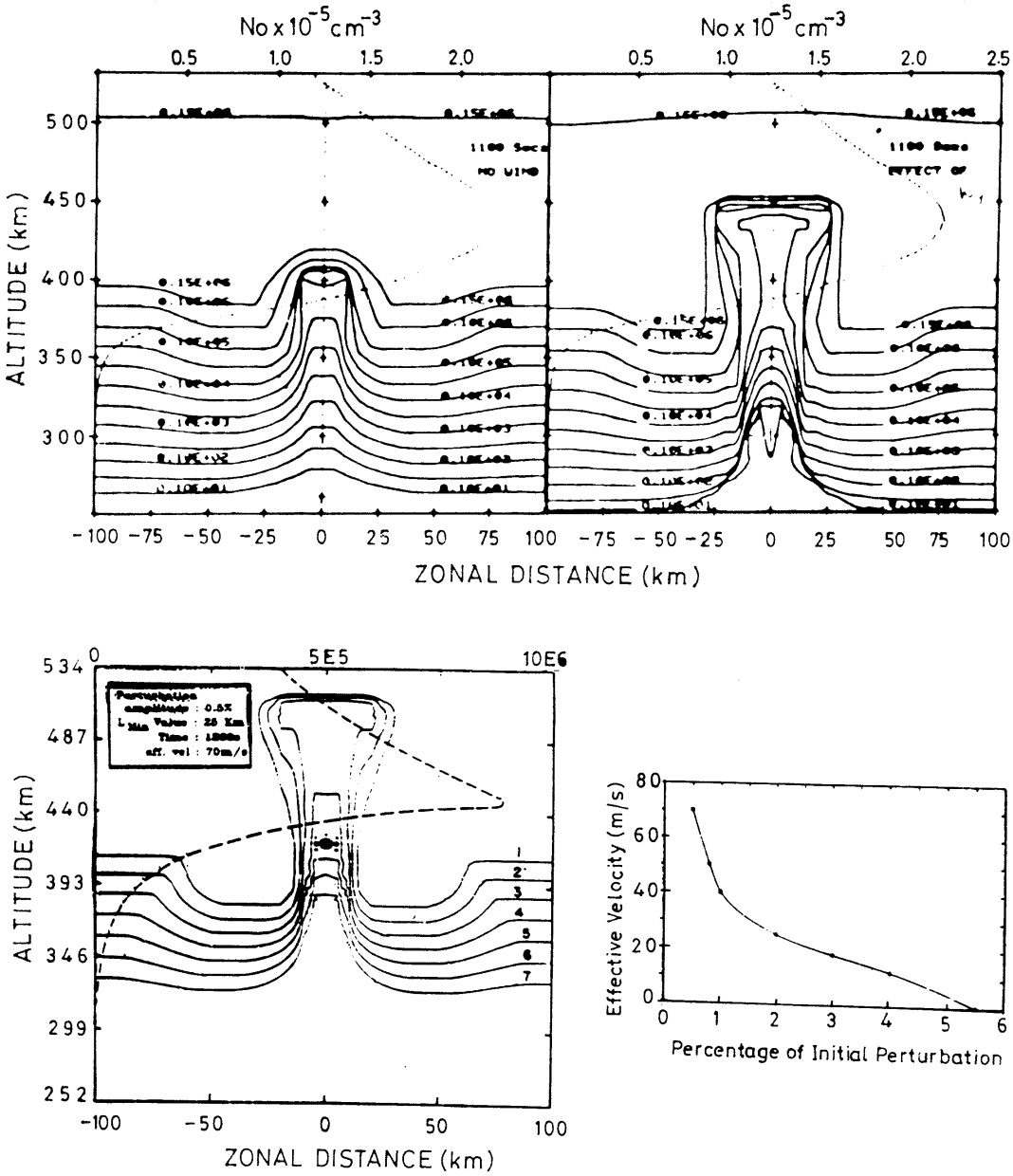

Fig 17 Results from nonlinear numerical simulation of ESF: *(top)* - Effects of vertically downward winds in altering the growth rate of the evolution of a plasma bubble - a comparative study with no wind and winds case[87]. *(bottom)* - Simulation studies revealing that the amplitude of the initial perturbation could be as small as 0.5% under favourable conditions i.e., when the effective vertical velocity ~ 70 ms^{-1} [89]

thermospheric circulation would enhance/inhibit ESF, depending upon the local time sector. During sunset hours, the disturbance dynamo electric field would inhibit EEJ, EIA and also the ESF through inhibition of prereversal enhancement of electric fields. Later in the night, the same field enhances both EIA and ESF mainly through prompt penetration of eastward electric field. However, there are examples as shown by Abdu *et al.*[95] from coordinated measurements from Brazilian and Indian longitudes which are in the night and day sectors for the existence of longitudinal structures in the disturbance dynamo field. While in the evening sector, over Brazil, the disturbance dynamo inhibited the evolution of ESF, no ESF was observed in the predawn Indian sector, contrary to the expectation. The competing nature of the neutral winds and the disturbance dynamo were thus highlighted.

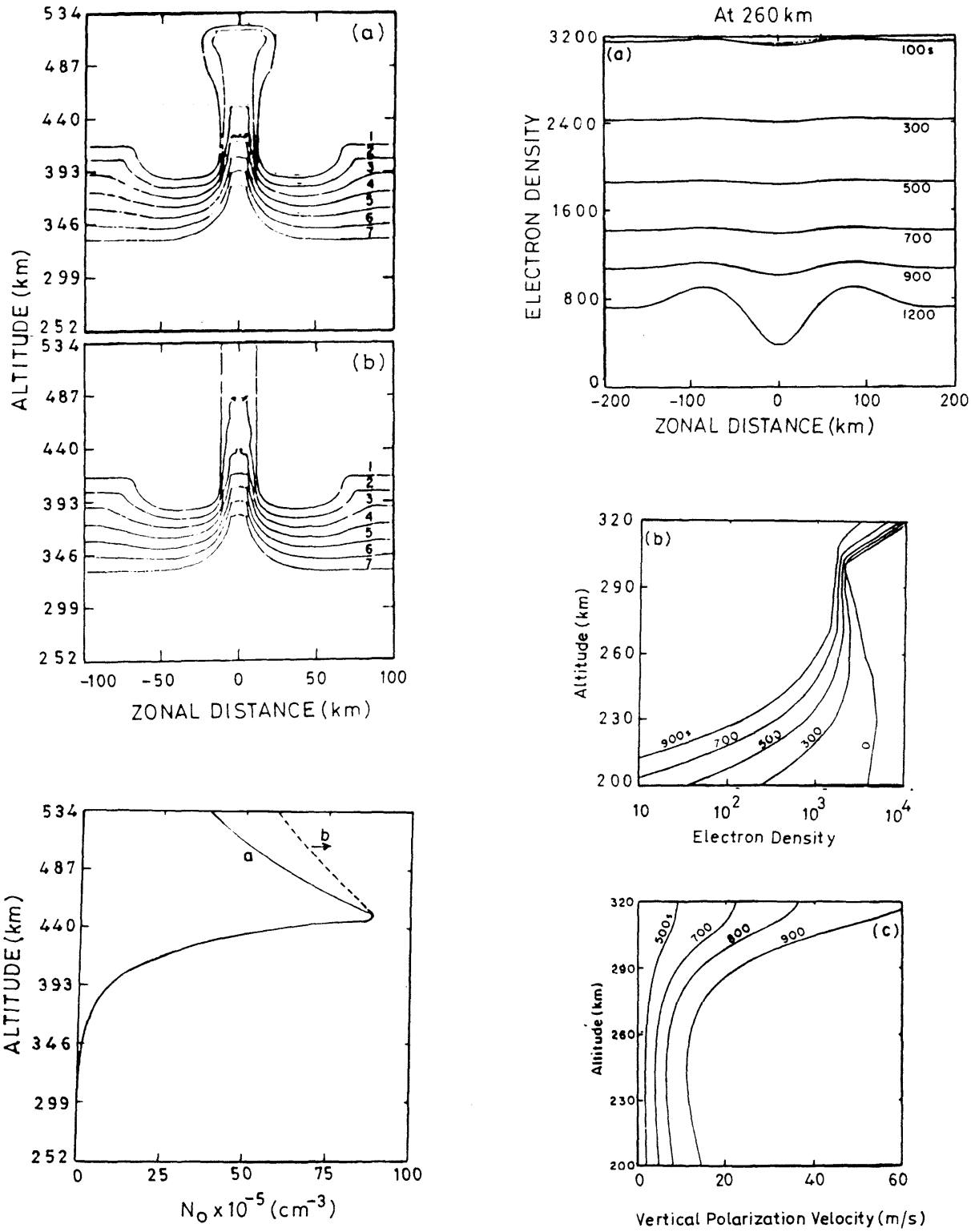

Fig. 17(*a*) - (*c*) *(left)* - The significant control of the topside electron density in the evolution of a plasma bubble. Smaller topside gradient enables pillar like bubbles, while the steeper topside gradient means a mushroom like bubble[90]. *(right)* - Successful explanation of the presence of plasma density irregularities in a negative gradient region by the effect of fringing fields[91].

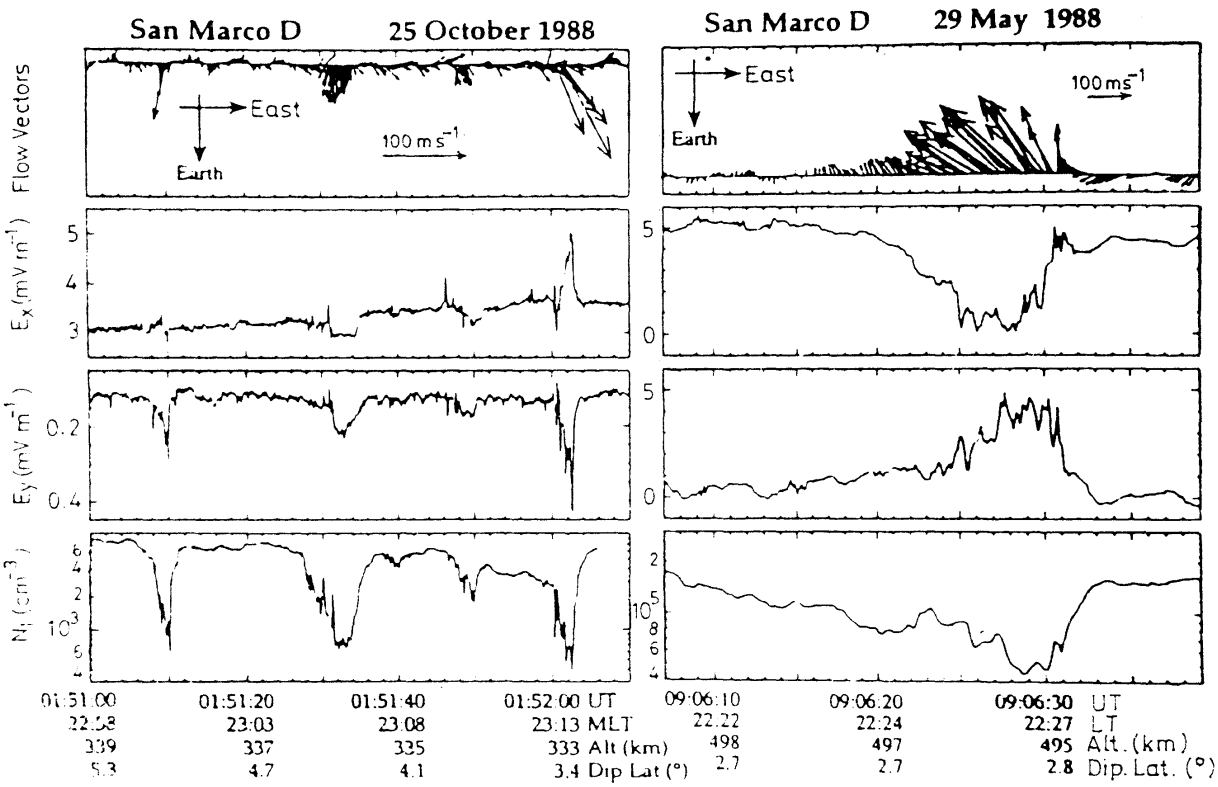

Fig. 18 *(left)* - Typical example of an updrafting channel with westward tilt; (E_x - eastward positive; E_y earthward positive); *(top panel)* - plasma flow vectors; *(bottom)* - ion density depicting the depletion; (2nd and 3rd panel) - electric field vectors; *(right)* - Downdrafting depletion channel[92].

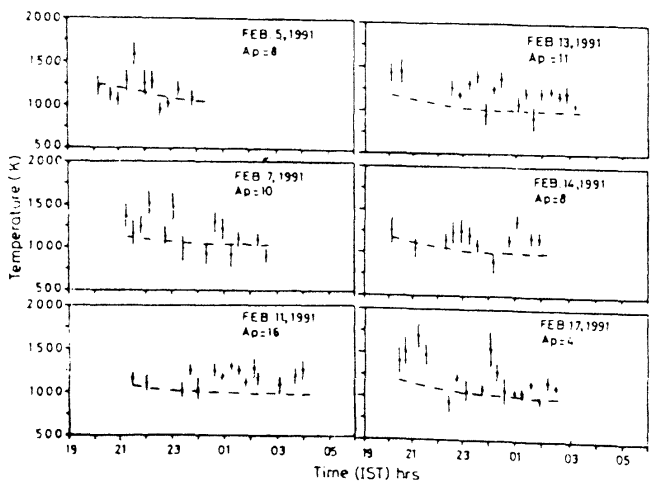

Fig. 19 Large scale variabilities in the spectroscopically measured neutral temperatures over Mt. Abu and their comparison with the MSIS model[99].

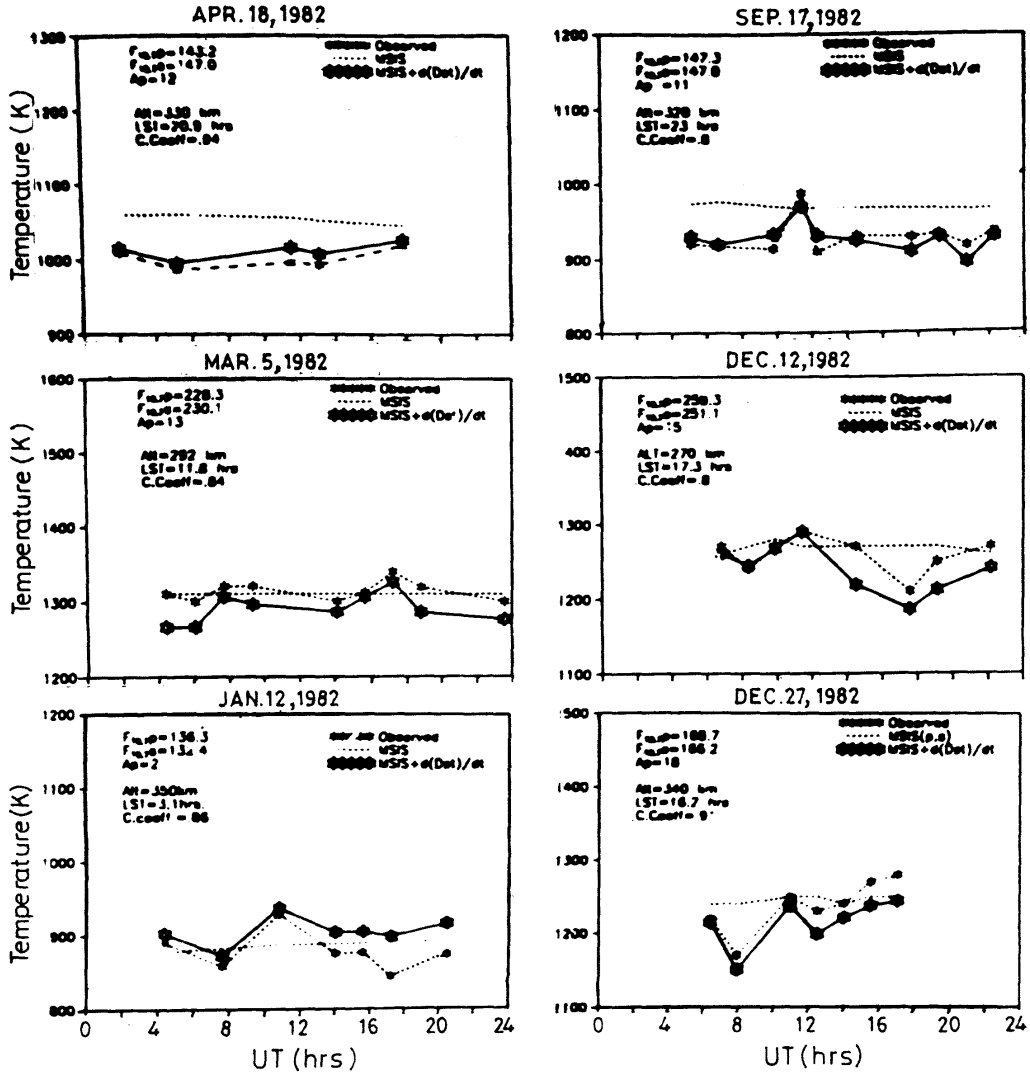

Fig. 20 Examples for the observed variabilities being explained by parameterising the D_{st} magnetic index and incorporating the same in the MSIS-90 model[11].

Representation of the Equatorial/Low Latitude Thermosphere-Ionosphere System by the Models

One of the primary objectives of any concerted study of TIS would be to be able to reasonably model the behaviour of the same for various geophysical conditions and eventually attain a reasonable level of predictability. The formulation of the atmospheric model had been evolving with time since some of the early attempts by Jacchia (1961, 1967, 1977) in *Smithsonian Astrophysical Observatory-Special Report* to the latest MSIS-90[96] model. On the other hand, the ionospheric models like empirical, semiempirical and analytical models have also been developed independently. The Semiempirical Ionospheric Model (SLIM), Fully Analytical Ionospheric Model (FAIM), Sheffield University Parameterized Ionospheric Model (SUPIM), are some of the widely used ionospheric models in addition to the International Reference Ionosphere (IRI) based mainly on measurements. One of the most recent models, viz., the Parameterised Ionospheric Model (PIM) fairly reproduces many of the ionospheric phenomena[97]. The major attempt to develop a Thermosphere-Ionosphere Electrodynamical Global Circulation Model (TIEGCM), the first of its kind[98], stands out in the modelling studies, by treating both the neutral and ionised constituents in a coupled self consistent manner. The complex nature of the above model with super computational requirements restricts the usage to a great extent. As mentioned during the discussion on MTM, the TIEGCM inspite of its comprehension, is not able to depict the equatorial region well including the prediction of the very well-known post sunset enhancement in the electric fields and the consequent

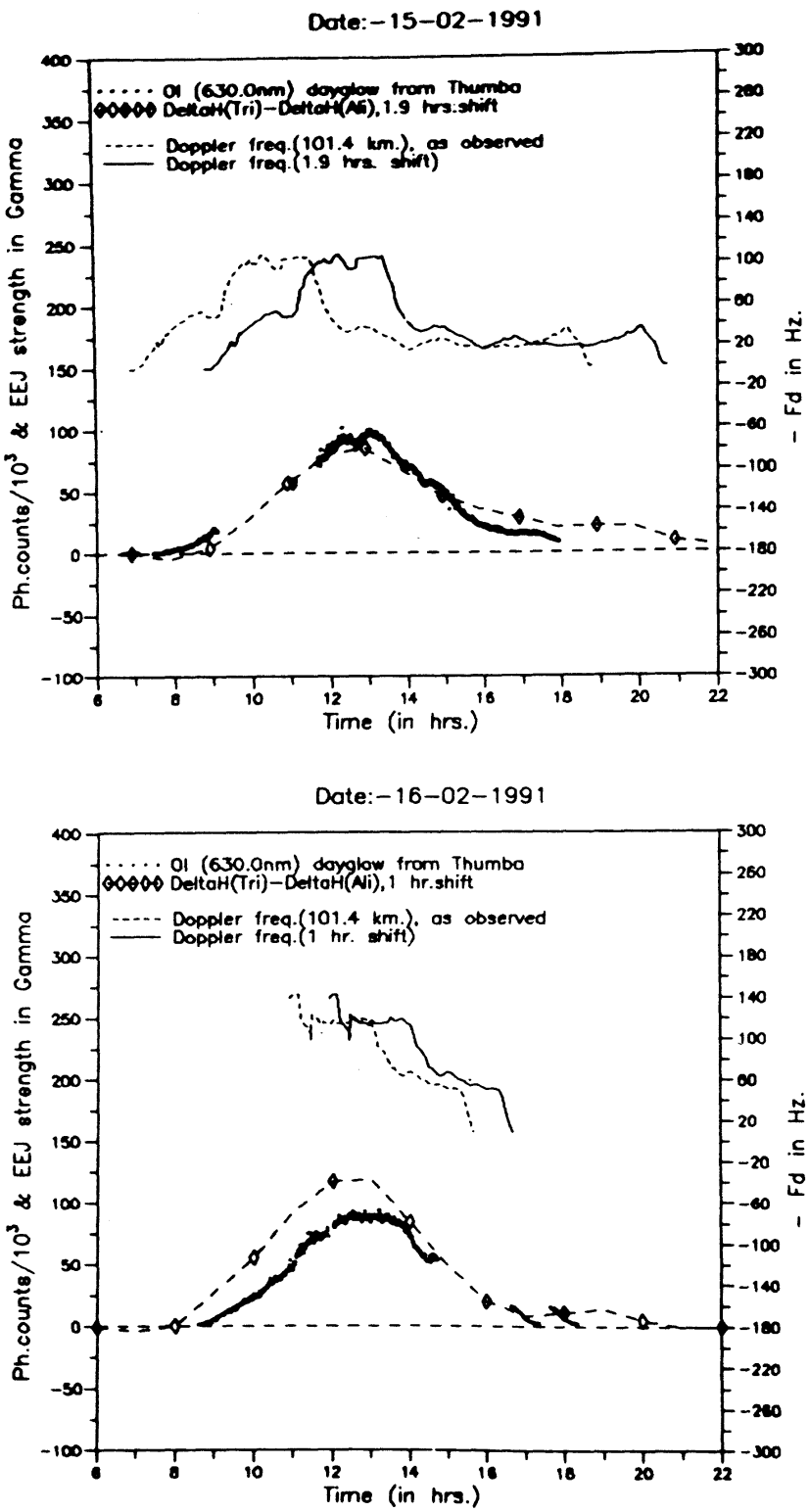

Fig. 21 The first direct experimental evidence for the imprint of the equatorial electrodynamical processes in the OI 630.0 nm daytime airglow. The one to one correspondence between the temporal variability in the electric field and the dayglow, with a time delay inversely proportional to the strength of the field[102] is shown.

lifting up of the F-region[60]. Efforts are on for the improvement of the said model.

The MSIS-90 model stands out amongst the various neutral thermosphere models, mainly because of its user friendliness. It has met with remarkable success over mid and high latitudes. However, this model too has significant limitation when it comes to low and equatorial latitudes, more so during magnetically disturbed periods. The measured thermospheric temperatures from low latitudes reveal significant deviations from the model values. It was believed that it could be due to geophysical processes like ETWA, MTM, etc. Large oscillatory features are seen on several occasions (Fig. 19)[99]. The model is not tuned to reproduce such variabilities and is infact designed to represent only the average conditions. There had been a debate in the recent times that the input to the MSIS model representing the different geophysical conditions in the form of magnetic indices like a_p and k_p may not be appropriate especially when it is applied to equatorial and low latitude, and, it was suggested that, instead the '**ring current**' index D_{st} could be used[100]. A method to parameterize the D_{st} index was also suggested therein. The

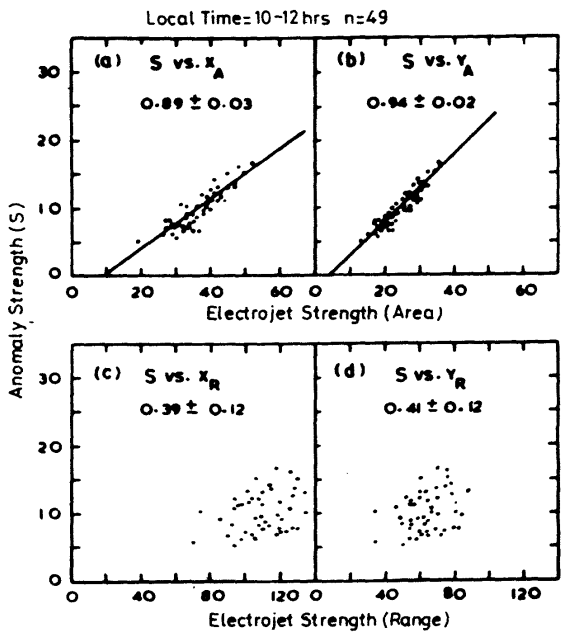

Fig. 22 One to one correlation between the integrated strength of the equatorial electrojet and the strength of the equatorial ionization anomaly[103].

significance of D_{st} from the point of view of wind measurements was demonstrated by Hernandez and Rofle[101] over mid latitudes. They had even shown a linear relation between the rate of change of D_{st} and the wind magnitude.

Detailed investigation using ground based spectroscopic as well as satellite data revealed a one to one correspondence between the time dalayed rate of change of D_{st} and the unaccounted difference in the model and measured temperature. The time delay had been shown to have a seasonal dependence with a minimum in summer (~ 11h) to a maximum (~ 16h) in winter months. The D_{st} index could now be parameterized after accounting for the local effects like ETWA and incorporated in the MSIS model. The model had been shown to reproduce the observed variabilities one to one[11] irrespective of the geomagnetic activity levels (Fig. 20). More detailed studies are called for in this direction.

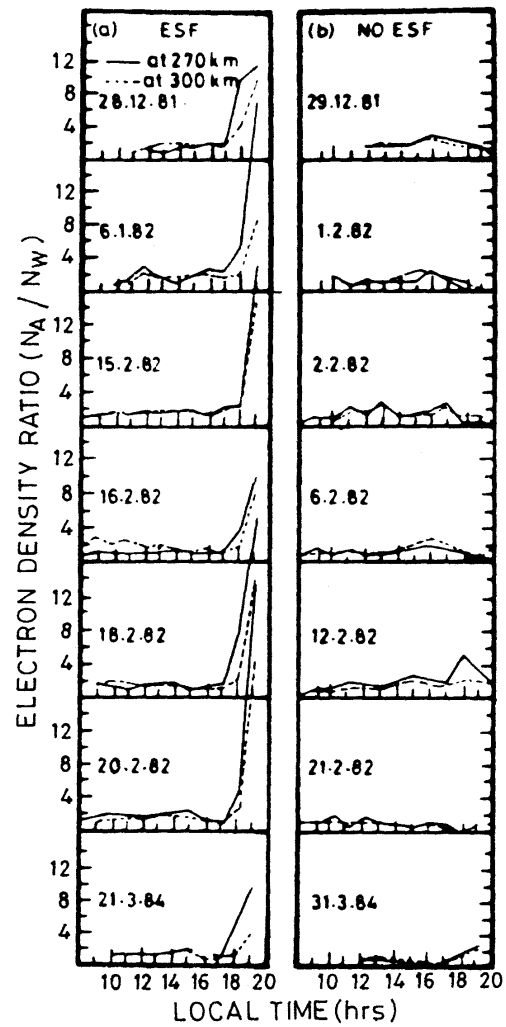

Fig. 23 The interrelation between the EIA and ESF - Strong anomaly means more probable occurrence of ESF[104,106]

Interrelation Between the Equatorial Processes

The unique equatorial/low latitude phenomena discussed above are interrelated amongst themselves. The global scale electric field in the east-west direction in the dynamo region driven essentially by the zonal winds is primarily responsible for the EEJ. It is the same zonal field that results in the uplifting of ionization above 150km over the dip equator only to diffuse along the geomagnetic field

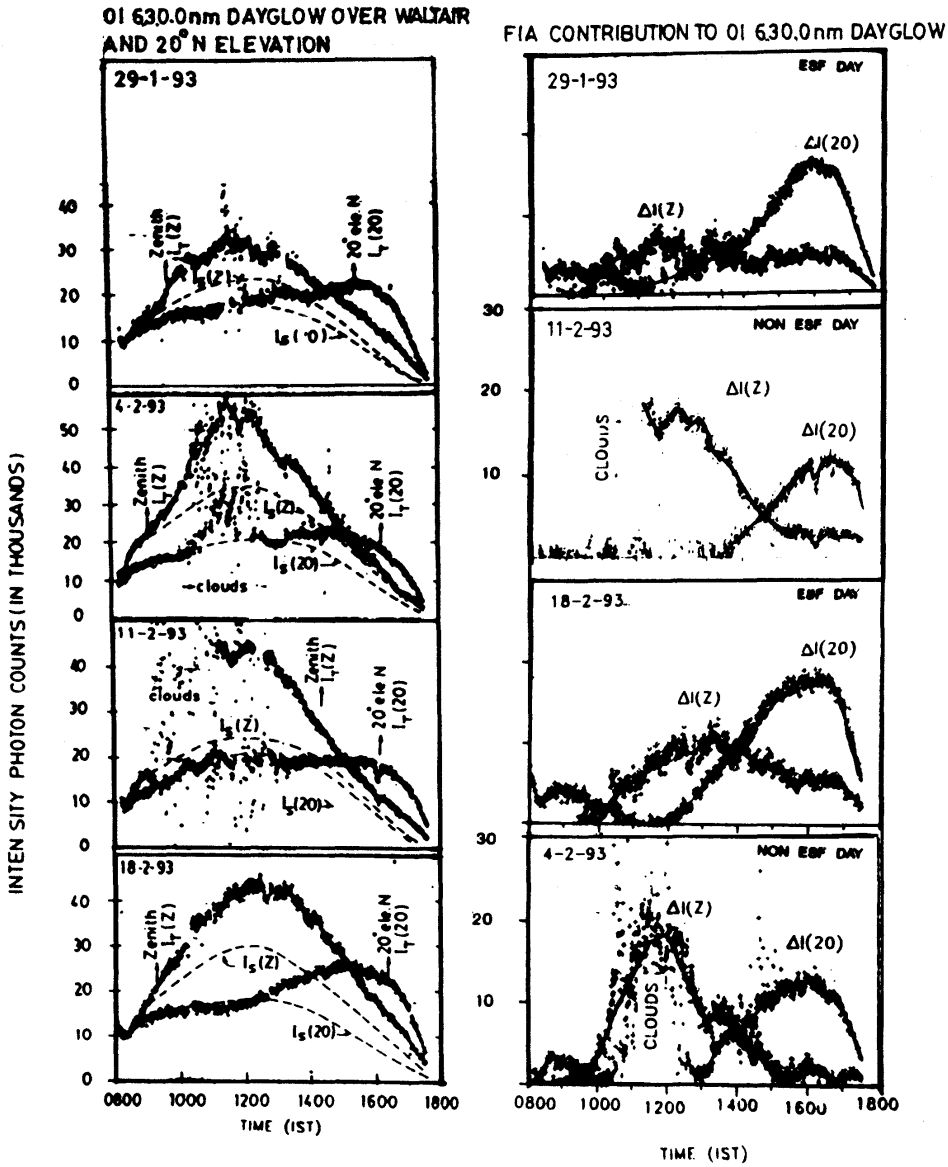

Fig. 24 Precursor to ESF in OI 630.0 nm dayglow based on the relation between EIA and ESF[107].

lines to higher latitudes resulting in the EIA. In fact, some of the recent result[102] from coordinated OI 630.0nm dayglow and VHF radar measurements from Thumba revealed that the thermospheric dayglow lags behind the electric field variations at the electrojet region, as obtained by the VHF radar. The time delay was shown to be inversely proportional to the strength of the EEJ or the driving electric field (Fig. 21). Raghavarao *et al.*[103] did provide a clear cut evidence for the one to one correspondence between the strength of the EIA and the time integrated EEJ (Fig. 22).

Notwithstanding this sort of a relation between the EEJ and the EIA, recent results revealed that the night time phenomenon of ESF has a strong relation to the daytime EIA. Raghavarao *et al.*[104] showed using simultaneous ionograms from two locations, one at Waltair (17.7° N, 83.3° E, 10.6° N dip lat.) and another over Ahmedabad that the ratio of electron densities at Ahmedabad and Waltair (N_w) at 270 and 300 km showed a steep increase by a factor of 8-30 around 1730h on ESF days and no such increase had been noticed on non-ESF days. These results have been confirmed also be Alex *et al.*[105,106] (Fig. 23). It had been further strengthened by the OI 630.0 nm dayglow measurements from Waltair operated in a bidirectional mode. Using the above logic Sridharan *et al.*[107] did succeed in getting a precursor to the phenomenon of ESF as early as 1600h. The above results (Fig. 24) reveal the close interrelation that prevails between ESF and EIA leaving the actual mechanism of the coupling open.

One of the possible means by which these two phenomena could be interrelated is through the intermediate geophysical phenomenon i.e., the equatorial temperature and wind anomaly. On strong EIA days, due to the combined effect of chemical heating and drag-effect, enhanced temperature and hence pressure bulges get developed at the crest location. These pressure bulges would have with them, the associated upward vertical winds. Downward winds have already been detected at the trough location by the DE-2 data[47]. It has been suggested that some sort of a circulation cell must be getting set up with equatorward flow in the upper thermosphere and a return flow at lower heights (Fig. 8*c*). Rocket experiments did show indications to this effect[108]. It had already been shown that vertically downward winds have the capability to enhance the growth rate of the primary R-T instability that evolves into an ESF event. This suggestion though definitely plausible and has the potential of explaining the day to day variability needs to be experimentally confirmed on a case by case basis. In the modelling front, improvement in the coupled thermosphere-ionosphere models should be able to bring out the interactive nature of these processes.

On the whole, it could be seen that the equatorial/low latitude Thermosphere-Ionosphere interactions manifest in a variety of ways ie., through various geophysical phenomena during magnetically quiet or disturbed periods. Programme like the Indian Solar-Terrestrial Energy Programme (I-STEP), the international programme like '**space-weather**' are expected to provide a better understanding for the interactive nature of the Thermosphere-Ionosphere System, in the years to come.

Acknowledgement

This work is supported by the Department of Space, Govt. of India.

References

1 R Sridharan *Curr Sci* **94** (1992) 588
2 V V Agashe, J H Sastri and R Sridharan *Adv Space Res in India, Diamond Jubilee Pub INSA (Ed.* R. K. Varma) (1994) 99
3 H Rishbeth *J atmos Terr Phys* **29** (1967) 225
4 H Rishbeth, S Ganguly and JCG Walker *J atmos Terr Phys* **40** (1978) 767
5 R Sridharan, S Gurubaran, R Raghavarao and R Suhasini *J atmos Terr Phys* **53** (1991) 515
6 M J Buansanto *J atmos Terr Phys* **48** (1986) 365
7 M J Buansanto *J atmos Terr Phys* **50** (1988) 373
8 S Gurubaran, R Sridharan and R Raghavarao *J atoms Terr Phys* **57** (1995) 1095
9 K L Miller, PG Richards and DG Torr *WITS Handbook* **2** (1979) 439
10 S Gurubaran and R Sridharan *J Geophys Res* **98** (1993)
11 T K Pant *Ph. D. Thesis* Gujarat Univ (1998)
12 B V Krishnamurthy, S S Hari and V V Somayajulu *J Geophys Res* **95** (1990) 4307
13 R Sekar and R Sridharan *J atmos Terr Phys* **54** (1992) 1197
14 H G Mayr, I Harris and N W Spencer *Rev Geophys Space Phys* **4** (1978) 539
15 A D Richmond *J atmos Terr Phys* **35** (1973*a*) 1083
16 A D Richmond *J atmos Terr Phys* **35** (1973*b*) 1105
17 B G Anandarao and R Raghavarao *Space Res* **XIX** (1979*a*) 283
18 B G Anandarao and R Raghavarao *J Geophys Res Lett* **92** (1987) 2514
19 C A Reddy and Devasia *J Geophys Res* **86** (1981) 5751
20 Untiedt *J Geophys Res* **72** (1967) 5799
21 R Raghavarao, R Sridharan and R Suhasini *J Geophys Res* **89** (1984) 11033
22 B V Krishnamurthy and K Sengupta *Planet Space Sci* **20** (1992) 371
23 R G Rastogi, H Chandra and S C Chakravarty *Proc Indian Acad Sci* **74** (1971) 62
24 R Raghavarao and B G Anandarao *Geophys Res Lett* **7** (1980) 357
25 V V Somayajulu, L Cherian, R Geetha and C Raghava Reddi *Geophys Res Lett* **20** (1993) 1443
26 R J Stenning *Proc IUGG Con Colarado* Boulder (1995)
27 V V Somayajula and Ligi Cherian *Curr Sci* **64** (1993) 579
28 M A Abdu *J atmos Terr Phys* **59** (1997) 1505
29 R D Rastogi and J A Klobuchar *J Geophys Res* **95** (1990) 19045
30 W B Hanson, D L Sterling and R F Woodman *J Geophys Res* **77** (1972) 5539
31 D N Anderson *J atmos Terr Phys* **55** (1993) 1661
32 R Sridharan, R Sekar and S Gurubaran *J atmos Terr Phys* **55** (1993) 1661
33 P Sharma and R Raghavarao *Can J Phys* **67** (1989) 166
34 R Raghavarao, R Sridharan, J H Sastri, V V Agashe, B C N Rao, P B and V V Somayajulu, *WITS Handbook* **1** (1988) p 48
35 T Araki, J H Allen and Y Araki *Planet Space Sci* **33** (1985) 11
36 T Kikuchi *J atmos Terr Phys* **91** (1986) 3101
37 J H Sastri, Y N Huang, T Shbata and T Okuzava *Geophys Res Lett* **22** (1995) 2645
38 M C Kelley, B G Fejer and C A Goncalez *Geophys Res Lett* **6** (1979) 301
39 R A Heelis *Rev Geophys* **26** (1988) 317
40 B G Fejer, M C Kelley C Senior, O J de La Beaujariere, J A Holt, C A Tapley, R Burnside, M A Abdu, J H A Sobral, R F Woodman, Y Kamide and R Lepping *J Geophys Res* **95** (1990) 2367
41 N Balan, G J Bailey, M A Abdu, K I Oyama, P G Rihards J Mac Doughall and I S Batista *J Geophys Res* **101** (1997) 15323
42 D N Anderson and R G Roble *J Geophys Res* **79** (1974) 5231
43 A D Richmond, E C Ridely and R G Roble *Geophys Res Lett* **19** (1992) 601

44 H Rishbeth *Planet Space Sci* **19** (1971) 357
45 A E Hedin and H G Mayr *J Geophys Res* **78** (1937) 1688
46 R Raghavarao, L E Wharton, N W Spencer, H G Mayr and L H Brace *Geophys Res Lett* **18** (1991) 1193
47 R Raghavarao, W R Hoegy, L E Wharton and N W Spencer *Geophys Res Lett* **20** (1993) 1023
48 R Raghavarao, R Suhasini, W R Hogey, G H Mayr and L Wharton *J atoms Terr Phys* (1998) (*To appear*)
49 T J Fuller-Rowell, M V Codrescu, B G Fejer, W Borer, F Marcos and D N Anderson *J atmos Terr Phys* **59** (1997) 1533
50 J A Greenspan *J atmos Terr Phys* **28** (1966) 739
51 G J Nelson and L L Cogger *J atmos Terr Phys* **33** (1971) 1711
52 R A Behnke and R M Harper *J Geophys Res* **78** (1973) 8222
53 N W Spencer, G R Carignan, H G Mayr, H B Neiman, R F Theis and L E Wharton *Geophys Res Lett* **6** (1979) 444
54 F A Herraro, N W Spencer and H G Mayr *Adv Space Res* **13** (1993) 202
55 H N Ranganatharao and J H Sastri *Annales Geophys* **12** (1994) 276
56 D K Bomgboye and J P McClure *Geophys Res Lett* **9** (1982) 457
57 J H Sastri H N Ranganatharao, V V Somayajulu and H Chandra *Geophys Res Lett* **21** (1994) 825
58 H G Mayr, I Harris, N W Spencer, A E Hendin, L E Wharton, H S Porter, J C G Walker and H C Carlson Jr *Geophys Res Lett* **6** (1979) 447
59 F A Herraro, H G Mayr and N W Spencer *J Geophys Res Lett* **88** (1983) 17225
60 C G Fesen *J Geophys Res* (1996) 26863
61 J M Forbes and H B Garrett *Geophys Res Lett* **5** (1978) 1013
62 G V Groves *J atmos Terr Phys* **44** (1982*a*) 111
63 G V Groves *J atmos Terr Phys* **44** (1982*b*) 281
64 B G Fejer, E R de Paula, S A Gonzalez and R F Woodman *J Geophys Res* **96** (1991) 13,901
65 G Haerendel *Max-Planck Inst Phys Astrophys Garching, Germany - Rep* (1973)
66 S L Ossakow *J atmos Terr Phys* **43** (1981) 437
67 M C Kelley, *The earth's ionosphere, plasma physics and electrodynamics. Int. Geophys Sr.* **43** (1989) Academic Press Sandiego California
68 T Maruyama and N Matuura *J Geophys Res* **89** (1984) 10903
69 R T Tsunoda *J Geophys Res* **90** (1985) 447
70 M A Abdu, I S Batista, and J H A Sobroal *J Geophys Res* **97** (1992) 14897
71 J Aarons *Space Sci Rev* ***63*** (1993) 209
72 H Rishbeth *Planet Space Sci* **19** (1971) 357
73 Rishbeth *J atmos Terr Phys* **59** (1997) 1873
74 R A Heelis, P C Kendal, R J Moffett, D W Windle and H Rishbeth *Planet Space Sci* **22** (1974) 743
75 D T Farley, E Bonelli, B G Fejer and M F Larson *J Geophys Res* **91** (1986) 13723
76 G Haerendal and J V Eccles *J Geophys Res* **97** (1992) 1181
77 J V Eccles *Low Lat Ionos Phys COSPAR Colloquia Sr* **7** (1994) 41
78 M C Kelley, M F Larsen, C A LaHoz and J P McClure *J Geophys Res* **86** (1981) 9087
79 C S Huang, M C Kelley and D E Hysell *J Geophys Res* **98** (1993) 15631
80 T L Aggson, N C Maynard, W B Hanson, and J K Saba *J Geophys Res* **97** (1992*a*) 2997
81 T L Aggson, W J Burke, N C Maynard, W B Hanson, P C Anderson, J A Slavin, W R Hogey and J L Saba *J Geophys Res* **97** (1992*b*) 858
82 B B Balsley, G Haerendal and R A Greenwald *J Geophys Res* **77** (1972) 5625
83 R Sekar and R Raghavarao *J atmos Terr Phys* **49** (1987) 981
84 P J Sultan *J Geophys Res* **101** (1996) 26875
85 S T Zalesak and S L Ossakow *J Geophys Res* **85** (1980) 2131
86 S T Zalesak, S L Ossakow and P K Chaturvedi *J Geophys Res* **87** (1982) 151
87 R Raghvarao, R Sekar and R Suhasini *Adv Space Res* ***12*** (1992) 227-230
88 R Sekar, R Suhasini and R Raghavarao *J Geophys Res* **99** (1994) 2205
89 R Sekar R Suhasini and R Raghavarao *Geophys Res Lett* **22** (1995) 885
90 R Sekar and R Raghavarao *Geophys Res Lett* **22** (1995) 3255
91 R Sekar, R Sridharan and R Raghavarao *J Geophys Res* **102**(1997) 20063
92 H Laasko, N C Maynard, R F Pfaff, T L Aggson, W R Coeley, P Janhunen and F A Herraro *J atmos Terr phys* (1997) 1625
93 A K Patra, P B Rao, V K Anandan and A R Jain *J atmos Terr Phys* **59** (1997) 1663
94 R Sekar *Proc IAGA Sym Uppsala Sweden* (1997)
95 M A Abdu, J H Sastri, J Mac Dougall, I S Batista and J H Sobral *Geophys Res Lett* **24** (1997) 1707
96 A E Hedin *et al. J Geophys Res* **95** (1991) 7995
97 RE Daniel, LD Brown, DN Anderson, MW Fox, PH Doherty, DT Decker, JJ Sojka, and RN Schunk *Rad Science* **30** (1995) 1499
98 A D Richmond, E C Ridley and R G Roble *Geophys Res Lett* **19** (1992) 601
99 S Gurubaran, R Sridharan, R Suhasini and K G Jani *J atmos Terr Phys* **57** (1995) 695
100 I Almer, E Illes-Almar, A Horvath, Z Kollath, D Bisikalo and T V Kasimenko *Adv Space Res* **12** (1992) 313
101 G Hernandez and R G Roble *J Geophys Res* **83** (1978) 5531
102 R Sridharan D Pallam Raju, V V Somayajulu, Alok Taori, D Chakrabarty and Raghavarao *J Geophys Res* (1998) (*In press*)
103 R Raghavarao, P Sharma and M R Sivaraman *Space Res* **XVII** (1978) 277
104 R Raghavarao, M Nageswararao, J Hanumath Sastri G D Vyas and M Sriramarao, *J Geophys Res* **93** (1988) 5959
105 S Alex, P V Koparkar and R G Rastogi *J atmos Terr Phys* **51** (1989) 371
106 P T Jayachandran, P Sri Ram, V V Somayajulu and P V S Ramarao, *Annales Geophys* **15** (1997) 255
107 R Sridharan, D Pallam Raju, R Raghavarao and PVS Ramarao *Geophys Res Lett* **21** (1994) 2797
108 R Sridharan, H Chandra, S R Das, R Sekar, H S Pallam Raju, D R Narayana Shike Raizada, R N Mishra, R Raghavarao, G D Vyas, P B Rao PVS Ramarao, V V Somayajulu, VV Babu and A D Danilov *J atmos Terr Phys* **59** (1997) 2051